Translational Relevance

Prognostic classification of heterogeneous diseases such as neuroblastoma remains challenging. In this study, a unique data-mining approach was applied for establishment of an accurate and robust gene expression classifier to predict clinical outcome of neuroblastoma patients. Using both published and unpublished microarray expression data of 933 primary neuroblastomas, a 42-gene classifier was developed and successfully validated. The powerful and independent prognostic value of the 42-gene classifier is shown using several lines of evidence. First, patients with divergent outcome were accurately classified. Second, multivariate analysis showed that the classifier is an independent prognostic factor, contributing to more accurate assessment of prognosis when considering the conventional risk factors alone. This was further confirmed within a subgroup of high-risk patients. Moreover, the excellent performance of the classifier across different expression platforms clearly shows its robustness. The presented gene selection procedure is suitable for the development of gene expression signatures in other cancer entities.

their effect on mRNA gene expression profiles, several microarray expression profiling studies have been undertaken to predict patient outcome in different cancer entities.

An important limitation of many published gene expression profiling studies is the lack of statistical power to identify markers and lack of independent validation. Typically, around 30,000 to 40,000 transcripts are tested, generating hundreds of thousands of data points for a relatively small subset of tumors (between 20 and 100). When such a high number of genes are evaluated as prognostic markers, there is a substantial chance that a random association between a gene and the prognostic classes is observed (9, 10). Consequently, many published studies do not classify patients better than chance due to lack of internal validation by repeated random sampling of training sets or external validation on independent samples. As such, there are a few inherent but often overlooked statistical issues, such as data overfitting, unstable gene lists, and lack of study power (11).

In this study, we established a prognostic 42-gene classifier for children with neuroblastoma by reanalysis of four published gene expression studies from four different microarray platforms comprising 582 patients in total (12–15). To facilitate data comparison across different platforms, probe annotations were updated with respect to the original publications. When available, clinical follow-up information was updated. All these aspects critically contribute to the success of our multigene signature. Successful validation of the multigene signature in four independent unpublished data sets shows its robust performance and platform independence.

Materials and Methods

Gene expression data sets. Four published studies were used for selecting the genes and building the prognostic classifier (phase 1 data sets), and four unpublished data sets were used as independent validation sets (phase 2 data sets).

The phase 1 data sets were downloaded either from the National Center for Biotechnology Information Gene Expression Omnibus (GSE2283 and GSE3960; refs. 14, 15) or from the European Bioinformatics Institute ArrayExpress database (E-TABM-38; ref. 13), or from the authors' Web site[10] (12).

A trained multigene correlation signature was validated on the four independent phase 2 data sets from which the 42 genes (when present) were extracted and standardized (per gene, the median value across the samples was subtracted followed by division by the SD of the gene): (*a*) hgu95av2 Affymetrix gene expression data from 106 neuroblastoma patients (validation set 1; 40 genes present), (*b*) hgu133plus2 Affymetrix gene expression data from 53 neuroblastoma patients (validation set 2; 40 genes present), (*c*) data set for 91 neuroblastoma patients obtained using an 11K custom Agilent oligonucleotide microarray (validation set 3; 41 genes present), and (*d*) Human Exon 1.0 ST Affymetrix expression data from 101 neuroblastoma patients (validation set 4; 42 genes present; standardized data of the 42-gene selection as well as clinical data are available in Supplementary Tables S1 and S2; Fig. 1).

For the remainder of the article, we will label the data sets according to the first author for the published phase 1 studies [Oberthuer (13), Wang (15), Berwanger (12), and Ohira (14)] and as validation sets 1, 2, 3, and 4 for the unpublished phase 2 studies.

Data preprocessing. To make the data from the different microarray platforms maximally comparable, annotation information of the probes was updated using the MatchMiner tool (16) for the custom-made cDNA or oligonucleotide arrays (12–14) and using the latest version of the R packages hgu95av2 and hgu133plus2 for the Affymetrix array data (15). Probe identification numbers were converted into gene symbols to enable straightforward comparison of the gene lists between the different studies. Throughout the text, the number of unique gene symbols (represented by one or more array probes) in each study is indicated.

Updated clinical information with regard to progression-free survival (PFS) and overall survival (OS) times was obtained from the authors (14, 15) or was publicly available (13). For the Berwanger and Ohira studies and validation set 1, only OS data were available.

[10] http://www.imt.uni-marburg.de/microarray/download.html

Patients were divided in two clearly defined risk groups. The low-risk subgroup was defined by stage I, II, or IVS without *MYCN* amplification, and the high-risk subgroup comprised patients with age of diagnosis >1 y with stage IV tumors (irrespective of *MYCN* status) or with stage II and III tumors with *MYCN* amplification. To develop our classifier, as many patients as possible from the four phase 1 data sets were divided in the two risk groups with maximally divergent clinical course (Table 1), that is, low-risk patients with PFS time (or OS time for Berwanger and Ohira data sets) of at least 1,000 d and high-risk patients that died from the disease. The patients that did not belong to the above-mentioned low- or high-risk subgroups were used as independent test set.

Statistical analysis. Identification and validation of prognostic classifiers (for each single phase 1 data set) were done by prediction analysis of microarray (PAM) classification with 10-times repeated 10-fold cross-validation in

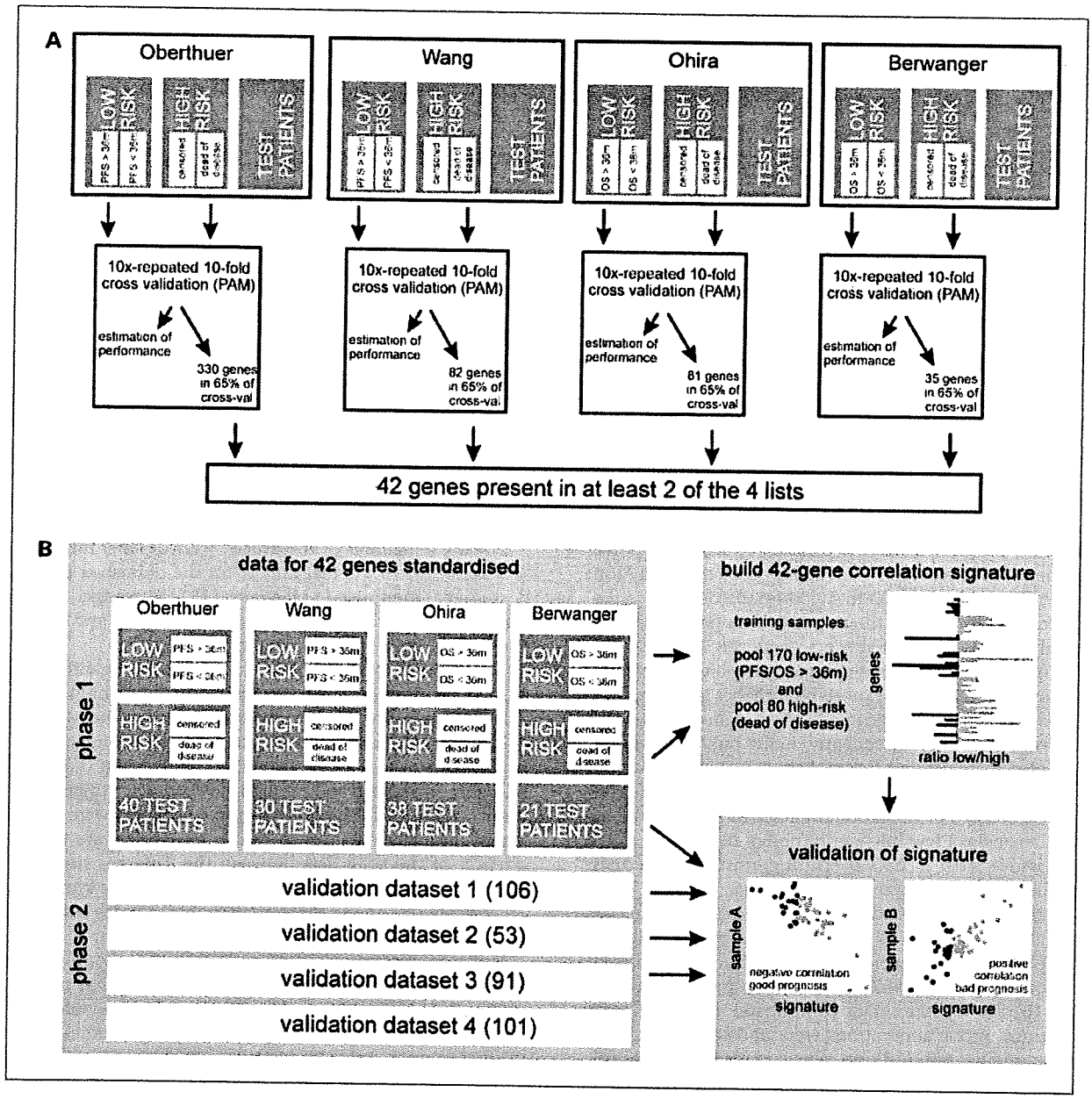

Fig. 1. Outline of the strategy used for prioritization of the 42 prognostic gene list (A) and construction of a 42-gene correlation signature and validation on independent test samples from phase 1 studies and phase 2 validation data sets (B). m, months.

Table 1. Published phase 1 studies used for training the classifier, with indication of the number of (training) samples, median OS or PFS (in months), and estimation of the performance of the study-specific PAM classifier for prediction of unfavorable outcome (OS)

	Berwanger	Oberthuer	Ohira	Wang
No. patients	94	251	136	101
No. low-risk training samples	22	87	43	18
No. high-risk training samples	13	25	20	22
Median OS/PFS (mo)	OS = 43	PFS = 55	OS = 46	PFS = 48
Specificity	0.955	0.977	0.814	1.000
Sensitivity	1.000	0.960	0.950	0.773
Negative predictive value	0.929	0.923	0.704	1.000
Positive predictive value	1.000	0.988	0.972	0.783
Accuracy	0.971	0.973	0.857	0.875
Performance (AUC)	0.977	0.969	0.882	0.886

the R statistical language using the Bioconductor package MCRestimate (Fig. 1A; refs. 13, 17). Forty-two genes were present in at least two of the four resulting gene lists.

A cross-platform gene signature was built using standardized expression data of the 42 genes (if present on the respective arrays, see Supplementary Data 2) from four published phase 1 studies. The correlation method was used to build and test a cross-platform prognostic signature (Fig. 1B). Log-transformed data were merged in one file (if more than one probe was present for a certain gene, the probe with the highest expression value was selected), and for each of the 42 genes, the mean expression value in low-risk neuroblastoma patients with PFS of at least 1,000 d was subtracted from the mean expression value in high-risk neuroblastoma patients that died of disease. For classification, the Pearson's correlation coefficient of the signature with the standardized expression values of independent test patients was calculated. Patients with a correlation coefficient below 0 were predicted to have good prognosis, whereas the other patients were predicted to have bad prognosis [according to Liu et al. (18)].

Kaplan-Meier survival analysis was done with the R survival package (R version 2.6.1). The area under the receiver operating characteristic curve (AUC) was used as a measure for the accuracy of the classifiers (ROCR R-package). Multivariate forward conditional logistic regression analysis was done using SPSS version 16.

Results

Gene prioritization for inclusion in a robust prognostic classifier. A complete 10-times repeated 10-fold cross-validation using the PAM algorithm (13, 19) was done on the training patients belonging to one of the two clearly defined risk groups from the four published phase 1 studies separately to identify robust prognostic markers (Fig. 1). This process was accompanied by determination of the classification accuracy, providing a first estimation of the utility of the expression data to predict outcome (Table 1).

For each data set, we selected the probes that were included in at least 65 of the 100 cross-validation gene lists, as these genes are likely to be the ones with the highest prognostic value as determined by Oberthuer et al. (13). The resulting prognostic gene lists from the four studies showed significant overlap (Table 2; Supplementary Data 1). Two genes were in common between three lists (i.e., *MYCN* and *NTRK1*), whereas 40 genes were in common between two lists. Thirty-two were previously reported in at least 1 of 10 published prognostic gene lists, of which only 10 were found in 2 or more published prognostic lists (12–14, 20–26). The occurrence of the 42 genes in at least two of the four lists makes them robust, platform-independent, prognostic markers.

Classification performance of the 42-gene list. Next, we investigated whether the 42-gene list is able to predict prognosis across different data sets. The classification performance was estimated in the different phase 1 data sets using a complete 10-times repeated 10-fold cross-validation method using all patients from the two clearly defined risk groups. For this analysis, it is important to note that not all 42 genes are present on all platforms; hence, the performance test was inherently done with a different number of genes for the different data sets (Supplementary Data 2). As already indicated, the 10-times repeated 10-fold cross-validation provides a good estimate for the classification performance using the expression data of the selected gene list.

As a reference, the 35-, 330-, 81-, and 82-gene lists obtained through single PAM analysis of each of the four phase 1 data sets were evaluated in the same way as the 42-gene list. The classification performance was also tested for a subset of 11 genes (from the 42-gene list) that were present on all four platforms. This analysis showed that all performance parameters for the 42-gene list are best or second best for all studies compared with the other gene lists, whereby the overall accuracy is highest for the 42-gene list subset (AUC = 0.935; Supplementary Data 2). This analysis also shows that the performance of a classifier built for

a given data set is not always best, which indicates the power and utility of our meta-analysis for the identification of a prognostic gene list by using expression data of 250 training samples (170 low risk and 80 high risk). When only 11 genes of the 42-gene list were selected that are present on all four platforms, the overall accuracy was lower due to loss in sensitivity and positive predictive value. The 42-gene classifier was also compared with two published classifiers (13, 27) and showed that the 42-gene classifier performs best.

Table 2. Genes that are in common between the 42-gene list and the different individual classifier gene lists (number of common genes in list/total number of genes in list)

	Berwanger (10/35)	Oberthuer (38/330)	Ohira (12/81)	Wang (26/82)	published lists
AHCY		−	−		2
AKR1C1		+		+	1
ARHGEF7		+	+		2
BIRC5	−		−		1
CADM1		+		+	0
CAMTA2		+		+	0
CDCA5	−	−			2
CDKN3		−		−	2
CLSTN1		+		+	1
DDC		+	+		1
DPYSL3		+	+		1
ECEL1		+	+		0
EPB41L3		+		+	0
EPHA5	+	+			1
EPN2		+		+	0
FYN			+	+	1
GNB1		+	+		1
HIVEP2		+		+	1
INPP1	+			+	1
MAP7	+	+			1
MAPT		+	+		1
MCM2		−		−	0
MRPL3		−		−	1
MYCN	−	−	−		4
NCAN		−		−	0
NME1	−	−			2
NRCAM		+		+	2
NTRK1		+	+	+	4
ODC1	−			−	1
PAICS		−		−	1
PLAGL1	+	+			1
PMP22		+		+	1
PRKACB		+		+	2
PRKCZ		+		+	1
PTN		+		+	1
PTPRN2		+	+		0
SCG2		+		+	1
SLC25A5		−		−	1
SNAPC1		−		−	0
TYMS		−		−	1
ULK2		+		+	0
WSB1	+	+			4

NOTE: The number of published prognostic gene lists (other than the four reanalyzed studies) in which these genes are found is indicated in the last column. −, associated with poor outcome; +, associated with favorable outcome.

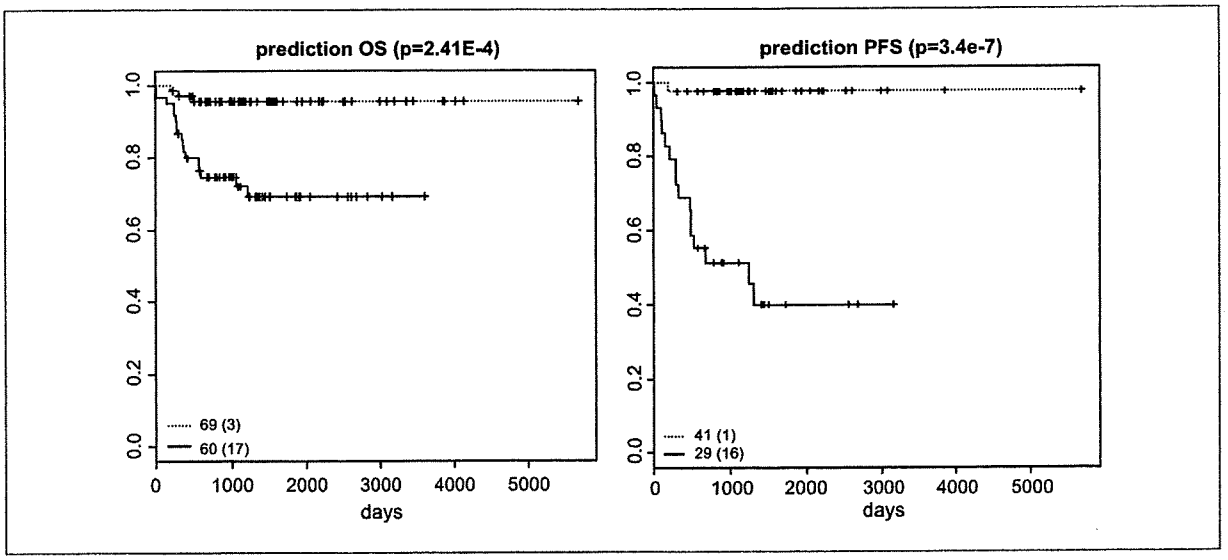

Fig. 2. Kaplan-Meier and log-rank analysis of 129 test patients (OS) and 70 test patients (PFS) from the four published phase 1 studies classified using the prognostic correlation signature. Legend, number of patients in predicted subgroups; between brackets, number of patients with event (relapse, progression, or death).

Validation of a cross-platform prognostic 42-gene correlation signature for neuroblastoma. A major disadvantage of the PAM classification method is the need for a training set of samples that are analyzed on the same gene expression measurement platform as the one used to evaluate the test samples. We therefore applied an alternative method to build a classifier based on the 42-gene list that can be used for completely independent data sets even on other platforms.

The prognostic signature is determined using 250 training samples from the four phase 1 studies. A 42-gene classification vector was created and tested using the correlation method (see Materials and Methods; Fig. 1).

First, the correlation signature was tested on the 129 test samples (patients not belonging to the low- and high-risk subgroup) from the four phase 1 studies and revealed a very high predictive power for OS (log-rank $P = 2.41E{-}4$) and PFS (log-rank $P = 3.40E{-}7$; Fig. 2).

Next, this correlation signature was evaluated on the four independent phase 2 data sets (351 patients), whereby the patients could be clearly separated into groups with significant differences in OS (log-rank $P = 2.17E{-}23$) and PFS (log-rank $P = 2.03E{-}21$; Fig. 3A). Kaplan-Meier analysis of patients stratified using known risk factors (i.e., age, stage, and *MYCN* gene status) showed that the correlation signature outperforms these risk factors ($P < 0.001$, except for *MYCN*-amplified samples; Supplementary Fig. S2). This was confirmed using multivariate logistic regression analysis evaluating age, stage, *MYCN* status, and the gene classifier, indicating that the 42-gene signature is an independent predictor for PFS and OS in the four phase 2 data sets as well as in the test samples of the phase 1 data sets (Table 3). Of note, whereas phase 2 data sets are representative of the general neuroblastoma population, test samples from the phase 1 data sets only represent intermediate risk patients.

As the different validation data sets include patients stratified using different risk stratification systems (Europe, United States, and Germany), we defined a common low- and high-risk group (Supplementary Data 3). As there was only 1 patient of 50 that died of disease within the common low-risk group of patients, we did not do Kaplan-Meier analysis. However, we could show that this single patient was classified in the high-molecular risk group using our classifier. Most interestingly, the correlation signature could partition patients within the common high-risk subgroup into groups with significant differences in OS and PFS (Fig. 3B) and was an independent prognostic marker (odds ratios, >4; Supplementary Table S4). To exclude that the significant survival differences in high-risk tumors is solely due to the effect of the *MYCN* amplification and related downstream *MYCN* signaling, we also tested the survival in high-risk tumors without *MYCN* amplification and could show that the classifier also significantly discriminates these patients with respect to outcome (Fig. 3C; Supplementary Table S4). In line with this, inspection of the 42-gene list indicated that not all 42-genes are related to *MYCN* amplification (Supplementary Data 4).

Discussion

In this study, we developed and validated a 42-gene prognostic classifier for children with neuroblastoma through a reanalysis strategy of published data complemented with gene expression data from 351 patients from

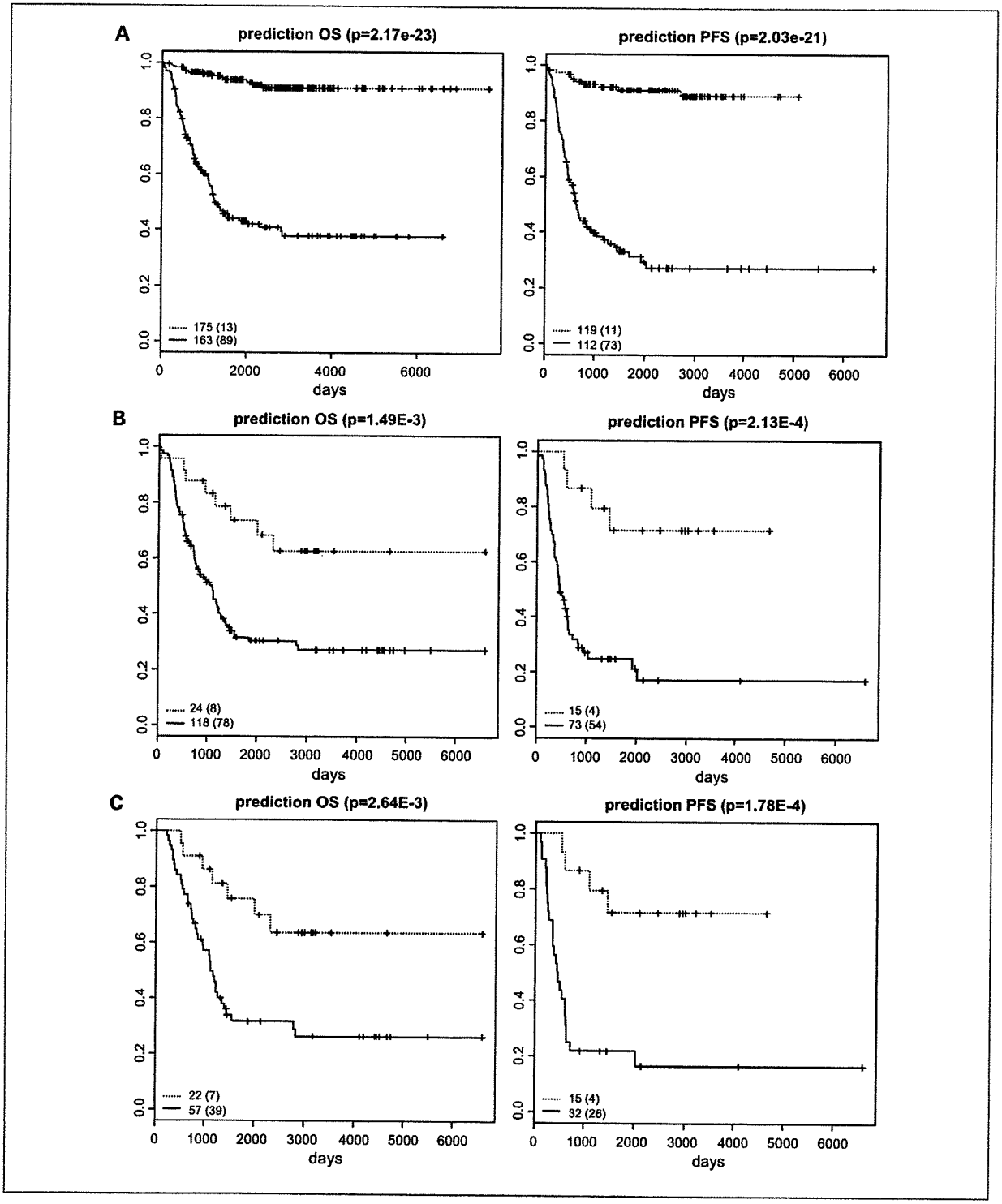

Fig. 3. Kaplan-Meier and log-rank analysis of the patients from four independent unpublished phase 2 validation data sets classified using the prognostic correlation signature for all patients together {5-y OS of 93.9% [95% confidence interval (95% CI), 90.2-97.6] for low molecular risk versus 43.1% (95% CI, 35.6-52.2) for high molecular risk and 5-y PFS of 91.1% (95% CI, 86.0-96.6) for low molecular risk versus 30.4% (95% CI, 22.1-41.8) for high molecular risk; A}, for the common high-risk subgroup (B), and for the common high-risk subgroup without MYCN amplification (C). Legend, number of patients in predicted subgroups; between brackets, number of patients with event (relapse, progression, or death).

Table 3. Multivariate logistic regression analysis (with correlation signature classification, MYCN status, International Neuroblastoma Staging System stage, and age at diagnosis; A) and sensitivity, specificity, and accuracy (AUC with 95% CI) results (follow-up time of at least 36 mo; B) for correlation signature prediction in the independent test samples from the phase 1 data sets and in the phase 2 validation data sets

A

		OS		PFS	
		P	OR (95% CI)	*P*	OR (95% CI)
Test samples from phase 1 data sets	Correlation signature	3.16E–2	5.11 (1.16-22.58)	3.12E–4	54.00 (6.17-472.41)
	MYCN amplification	7.80E–5	21.50 (4.69-98.54)	1.26E–1	—
	Stage (IV versus other)	1.80E–1	—	2.65E–1	—
	age (<1 or >1 y)	1.52E–1	—	8.65E–1	—
Phase 2 validation data sets	Correlation signature	9.07E–7	7.02 (3.23-15.28)	1.1E–14	16.45 (8.09-33.48)
	MYCN amplification	4.19E–2	2.23 (1.03-4.84)	3.13E–1	—
	Stage (IV versus other)	1.35E–2	2.50 (1.21-5.16)	2.16E–1	—
	age (<1 or >1 y)	1.45E–4	4.14 (1.99-3.66)	1.1E–4	4.18 (2.03-8.64)

B

	Test samples from phase 1 data sets	Phase 2 validation data sets
Sensitivity OS	17/20 = 0.85	89/102 = 0.87
Specificity OS	41/67 = 0.61	140/195 = 0.72
Performance, AUC (95% CI), OS	0.731 (0.612-0.850)	0.795 (0.742-0.849)
Sensitivity PFS	16/17 = 0.94	93/110 = 0.85
Specificity PFS	27/35 = 0.77	95/119 = 0.80
Performance, AUC (95% CI), PFS	0.856 (0.748-0.964)	0.822 (0.764-0.879)

NOTE: —, not analyzed.
Abbreviation: OR, odds ratio.

four unpublished data sets (Fig. 1). To accomplish this, four published microarray studies comprising >500 neuroblastoma patients were reanalyzed generating four new prognostic gene lists with a high overlap of genes between them. Comparison of the genes in the classifiers showed that 42 unique genes were present in at least two of the four lists. Not surprisingly, this set of 42 predictor genes contains numerous genes that have been reported in the context of neuroblastoma (e.g., *MYCN, NTRK1, NME1, CADM1, FYN, ODC1,* and *WSB1*). The finding of these genes in at least two independent studies indicates their robustness as prognostic markers. Comparison of the performance of the 42-gene list with the lists that were generated on the individual phase 1 studies and with two published prognostic gene lists (13, 27) showed that the classifier based on the 42-gene list has the highest overall accuracy while using the lowest number of genes. However, we have to keep in mind that this observed superiority of the 42-gene set might in part be due to the fact that, for some of the other gene lists, a large proportion of genes were not present on the platform (Supplementary Table S3).

The high prognostic classification performance of the 42-gene list is undoubtedly due to our unique reanalysis approach. First, annotations of the probes on the different platforms were updated according to the latest genome build. Second, a uniform risk definition was applied to select training patients across the different studies. Only patients with maximally divergent courses were used for training. Third, the same powerful algorithm with built-in cross-validation was used for identification of prognostic genes in four major published data sets, enabling the generation of relatively stable prognostic gene lists with high overlap.

This list of 42 prognostic genes was used to build a cross-platform classification signature. As the PAM algorithm is not suitable for cross-platform classification, we used a more intuitive, alternative method for building a 42-gene classifier. In this study, we generated a prognostic correlation signature based on expression data of the 42 genes in 250 training samples of the four phase 1 data sets. The signature was subsequently applied on independent test samples from the phase 1 data sets and on four independent and unpublished phase 2 data sets, generated on different expression profiling platforms, totaling 480 patients. The excellent prognostic performance of the 42-gene list (Table 3) further shows the validity of our meta-analysis approach and the utility of the recognized prognostic markers for neuroblastoma. The classifier predicts overall (OS) and PFS for the patients from the four phase 2 studies as well as for the test patients from the phase 1 studies (which could not be unequivocally classified in the low- or high-risk subgroups using known risk factors) with high sensitivity and specificity (Table 3). Importantly, the classifier was shown to be an independent predictor for both PFS and OS when stratifying for known risk factors such as age, stage, and *MYCN* status. Indeed, the 42-gene list does not only contain *MYCN*-regulated genes and, thus, not only reflects the *MYCN* copy number status of the samples. This is further substantiated by the excellent performance of the classifier in the high-risk neuroblastoma patients without *MYCN* amplification.

Thus far, this is the largest prognostic meta-analysis study in neuroblastoma, totaling >900 patients, including 351 patients from four independent and unpublished validation data sets. In contrast to other studies on neuroblastoma gene expression classifiers (13, 14, 21, 25, 27, 28), we could show an excellent performance of our classifier on these four independent data sets involving patients from different risk protocols from Germany, Europe, and United States by using a smaller gene set and a more intuitive classification method.

This survival classifier will definitely help to identify patients with increased risk in the current risk groups and to make a better choice of risk-related therapy. For example, low-risk patients with high molecular risk might benefit from more aggressive treatment protocols, whereas more intensive follow-up and new experimental therapies might be considered for high-risk patients with high molecular risk.

In conclusion, we applied a unique meta-analysis strategy for the identification of a robust set of 42 prognostic genes for outcome prediction in neuroblastoma. Furthermore, we propose a prognostic gene signature that is significantly associated with outcome prediction in neuroblastoma samples from independent studies using different technological platforms, making it a useful and practical classifier for risk stratification in neuroblastoma patients. The signature remains to be tested in a prospective clinical validation. The low number of genes makes this signature very well suited for cost-effective and fast PCR-based analysis, requiring only minimal amounts of tumor material, as exemplified by a recently published quantitative PCR study in which a 59-gene classifier containing the 42 genes from this study was trained, tested, and independently validated on a large cohort of patients (29). The outlined strategy for robust selection of prognostic markers and the use of a cross-platform correlation signature have wide application potential in other cancer entities.

In the search of an optimal prognostic classifier, it could prove useful to do an integrated analysis to determine the combined prognostic power of a mRNA gene expression signature along with gene copy number levels, microRNA gene expression patterns, and epigenetic modifications.

Disclosure of Potential Conflicts of Interest

No potential conflicts of interest were disclosed.

Acknowledgments

We thank Vincent Detours for critical reading of the manuscript and helpful suggestions and the Children's Oncology group.

Grant Support

European Community under the FP6 (project: STREP: EET-pipeline, number: 037260). This article presents research results of the Belgian program of Interuniversity Poles of Attraction, initiated by the Belgian State, Prime Minister's Office, Science Policy Programming. K. De Preter is a postdoctoral researcher with the Fund for Scientific Research-Flanders. J. Vermeulen is a Ph.D. student with the Belgian Kid's Fund and the Fondation pour la recherche Nuovo-Soldati. This study was sponsored by the 'Kinderkankerfonds,' the 'Stichting tegen Kanker,' the Fund for Scientific Research and BOF-UGent, and the fondation Fournier Majoie pour l'innovation.

The costs of publication of this article were defrayed in part by the payment of page charges. This article must therefore be hereby marked *advertisement* in accordance with 18 U.S.C. Section 1734 solely to indicate this fact.

Received 09/27/2009; revised 11/27/2009; accepted 12/22/2009; published OnlineFirst 02/23/2010.

References

1. Brodeur GM, Fong CT, Morita M, Griffith R, Hayes FA, Seeger RC. Molecular analysis and clinical significance of N-myc amplification and chromosome 1p monosomy in human neuroblastomas. Prog Clin Biol Res 1988;271:3–15.
2. Brodeur GM, Pritchard J, Berthold F, et al. Revisions of the international criteria for neuroblastoma diagnosis, staging, and response to treatment. J Clin Oncol 1993;11:1466–77.
3. Brodeur GM, Seeger RC, Schwab M, Varmus HE, Bishop JM. Amplification of N-myc in untreated human neuroblastomas correlates with advanced disease stage. Science 1984;224:1121–4.
4. Evans AE, D'Angio GJ, Randolph J. A proposed staging for children with neuroblastoma. Children's cancer study group A. Cancer 1971; 27:374–8.
5. Look AT, Hayes FA, Nitschke R, McWilliams NB, Green AA. Cellular DNA content as a predictor of response to chemotherapy in infants with unresectable neuroblastoma. N Engl J Med 1984;311:231–5.

6. Maris JM. The biologic basis for neuroblastoma heterogeneity and risk stratification. Curr Opin Pediatr 2005;17:7–13.
7. Shimada H, Ambros IM, Dehner LP, et al. The International Neuroblastoma Pathology Classification (the Shimada system). Cancer 1999;86:364–72.
8. Cohn SL, Pearson AD, London WB, et al. The International Neuroblastoma Risk Group (INRG) classification system: an INRG Task Force report. J Clin Oncol 2009;27:289–97.
9. Simon R. Diagnostic and prognostic prediction using gene expression profiles in high-dimensional microarray data. Br J Cancer 2003; 89:1599–604.
10. Tinker AV, Boussioutas A, Bowtell DD. The challenges of gene expression microarrays for the study of human cancer. Cancer Cell 2006;9:333–9.
11. Michiels S, Koscielny S, Hill C. Prediction of cancer outcome with microarrays: a multiple random validation strategy. Lancet 2005; 365:488–92.
12. Berwanger B, Hartmann O, Bergmann E, et al. Loss of a FYN-regulated differentiation and growth arrest pathway in advanced stage neuroblastoma. Cancer Cell 2002;2:377–86.
13. Oberthuer A, Berthold F, Warnat P, et al. Customized oligonucleotide microarray gene expression-based classification of neuroblastoma patients outperforms current clinical risk stratification. J Clin Oncol 2006;24:5070–8.
14. Ohira M, Oba S, Nakamura Y, et al. Expression profiling using a tumor-specific cDNA microarray predicts the prognosis of intermediate risk neuroblastomas. Cancer Cell 2005;7:337–50.
15. Wang Q, Diskin S, Rappaport E, et al. Integrative genomics identifies distinct molecular classes of neuroblastoma and shows that multiple genes are targeted by regional alterations in DNA copy number. Cancer Res 2006;66:6050–62.
16. Bussey KJ, Kane D, Sunshine M, et al. MatchMiner: a tool for batch navigation among gene and gene product identifiers. Genome Biol 2003;4:R27.
17. Ruschhaupt M, Huber W, Poustka A, Mansmann U. A compendium to ensure computational reproducibility in high-dimensional classification tasks. Stat Appl Genet Mol Biol 2004;3:Article37.
18. Liu R, Wang X, Chen GY, et al. The prognostic role of a gene signature from tumorigenic breast-cancer cells. N Engl J Med 2007;356:217–26.
19. Tibshirani R, Hastie T, Narasimhan B, Chu G. Diagnosis of multiple cancer types by shrunken centroids of gene expression. Proc Natl Acad Sci U S A 2002;99:6567–72.
20. Yamanaka Y, Hamazaki Y, Sato Y, et al. Maturational sequence of neuroblastoma revealed by molecular analysis on cDNA microarrays. Int J Oncol 2002;21:803–7.
21. Wei JS, Greer BT, Westermann F, et al. Prediction of clinical outcome using gene expression profiling and artificial neural networks for patients with neuroblastoma. Cancer Res 2004;64: 6883–91.
22. Takita J, Ishii M, Tsutsumi S, et al. Gene expression profiling and identification of novel prognostic marker genes in neuroblastoma. Genes Chromosomes Cancer 2004;40:120–32.
23. Ohira M, Morohashi A, Inuzuka H, et al. Expression profiling and characterization of 4200 genes cloned from primary neuroblastomas: identification of 305 genes differentially expressed between favorable and unfavorable subsets. Oncogene 2003;22: 5525–36.
24. Hiyama E, Hiyama K, Yamaoka H, Sueda T, Reynolds CP, Yokoyama T. Expression profiling of favorable and unfavorable neuroblastomas. Pediatr Surg Int 2004;20:33–8.
25. Asgharzadeh S, Pique-Regi R, Sposto R, et al. Prognostic significance of gene expression profiles of metastatic neuroblastomas lacking MYCN gene amplification. J Natl Cancer Inst 2006;98: 1193–203.
26. Abel F, Sjoberg RM, Nilsson S, Kogner P, Martinsson T. Imbalance of the mitochondrial pro- and anti-apoptotic mediators in neuroblastoma tumours with unfavourable biology. Eur J Cancer 2005; 41:635–46.
27. Chen QR, Song YK, Wei JS, et al. An integrated cross-platform prognosis study on neuroblastoma patients. Genomics 2008;92: 195–203.
28. Warnat P, Oberthuer A, Fischer M, Westermann F, Eils R, Brors B. Cross-study analysis of gene expression data for intermediate neuroblastoma identifies two biological subtypes. BMC Cancer 2007;7:89.
29. Vermeulen J, De Preter K, Naranjo A, et al. Predicting outcomes for children with neuroblastoma using a multigene-expression signature: a retrospective SIOPEN/COG/GPOH study. Lancet Oncol 2009;10: 663–71.

Cancer Science
The official journal of the Japanese Cancer Association JCA

Prolonged low-dose administration of the cyclooxygenase-2 inhibitor celecoxib enhances the antitumor activity of irinotecan against neuroblastoma xenografts

Michio Kaneko,[1] Setsuko Kaneko and Kenshi Suzuki

Department of Pediatric Surgery, Graduate School of Comprehensive Human Sciences, University of Tsukuba, Tsukuba, Japan

(Received February 18, 2009/Revised June 30, 2009/Accepted July 02, 2009/Online publication August 6, 2009)

Cyclooxygenase (COX)-2 is overexpressed in many human tumors including neuroblastoma (NB) and promotes tumor progression. We evaluated the antitumor effect of irinotecan (CPT-11) treatment combined with prolonged very low-dose administration of celecoxib, a selective COX-2 inhibitor, against three human NB xenografts, TNB9, TS-N-2*nu*, and TS-N-5*nu*. In addition, the effects of the celecoxib-combined treatment were examined on tumor cell proliferation, apoptosis, angiogenesis, and expression of vascular endothelial growth factor and apoptosis-related proteins in xenografts. Celecoxib administered daily at 5 mg/kg body weight/day could not prevent the growth of any of the NB xenografts. However, the combination of daily low-dose CPT-11 (5.9 mg/kg body weight/day) and simultaneous very low-dose celecoxib resulted in highly significant suppression of tumor growth in all three xenografts ($P < 0.001$) compared not only with low-dose CPT-11 therapy alone but also with the combination therapy of intermittent conventional-dose CPT-11 (59 mg/kg body weight) and celecoxib accompanied by decreased proliferation and increased induction of apoptosis in tumor cells. Induction of apoptosis by CPT-11 with and without celecoxib was associated with the up-regulation of Bax expression and the down-regulation of Bcl-2 expression. The enhanced antitumor effect of the combination of the two drugs against the NB xenografts might be partially COX-2-independent and was probably mediated through multiple factors including diminished expression of VEGF and activation of the caspase-dependent mitochondrial apoptosis pathway. These findings demonstrate that prolonged low-dose CPT-11 treatment combined with very low-dose celecoxib shows promising antitumor activity through the blockage of multiple critical targets related to NB tumor cell survival and proliferation. (*Cancer Sci* 2009; 100: 2193–2201)

Neuroblastoma (NB) is one of the most common malignant childhood solid tumors. There have been significant advances in the treatment of NB with intensive induction and consolidation chemotherapy regimens. However, the treatment results for patients aged 1 year or older with disseminated disease and for those with *MYCN*-amplified NB are still unsatisfactory. Among the antitumor drugs with therapeutic activity, irinotecan (CPT-11), a semisynthetic derivative of camptothecin, is promising for NB treatment.[1–4] Recently, phase II studies of CPT-11 in children with refractory solid tumors including NB and with relapsed or refractory NB concluded that CPT-11 treatment was well tolerated, but not effective as a single agent, with the possible exception of its use against medulloblastoma.[5,6] We have previously shown that CPT-11 is highly effective against human NB xenografts when administered at a conventional dose ($LD_{50} \times 1/3$ per dose) at 4-day intervals according to the protocol of Battelle Columbus laboratories, and that a daily low-dose ($LD_{50} \times 1/30$ per dose) administration is equally or more effective than conventional-dose intermittent CPT-11 treatment.[7] However, treatment with CPT-11 alone could not eradicate the tumor in mice.

Cyclooxygenases (COXs) catalyze the conversion of arachidonic acid to prostaglandins and consist of two isoenzymes, the constitutive COX-1 and the inducible COX-2. COX-1 is constitutively and ubiquitously expressed in most tissues, whereas COX-2 is induced by various inflammatory and mitogenic stimuli such as cytokines and growth factors.[8] Recent studies suggest that COX-2 promotes tumorigenesis by stimulating cancer cell proliferation, increasing tumor angiogenesis, preventing cancer cell apoptosis, and enhancing tumor metastasis.[9–13] COX-2 is overexpressed in various human tumors including NB.[14,15] Besides its anti-inflammatory and analgesic effects, selective COX-2 inhibitors have been shown to exert antitumor activity through many mechanisms, especially via anti-angiogenic and pro-apoptotic effects.[15–18] We evaluated the inhibitory effect of very low-dose celecoxib, a selective COX-2 inhibitor, on tumor growth combined with prolonged low-dose or intermittent conventional-dose CPT-11 treatment against three neuroblastoma xenografts in mice. We further investigated the *in vivo* effects of combined treatment involving low-dose CPT-11 and celecoxib on tumor cell proliferation, apoptosis, angiogenesis, and the expression of vascular endothelial growth factor (VEGF) and apoptosis-related proteins in xenografts, as well as the *in vitro* effects of low concentrations of celecoxib on cytotoxic activity of SN-38, an active metabolite of CPT-11, and expression of caspases in NB cell lines.

Materials and Methods

Animals and human NB xenografts. Human NB xenografts designated TNB9, TS-N-2*nu*, and TS-N-5*nu* were derived from stage 4 NBs with 80, 13, and more than 100 copies of the *MYCN* amplification developed in the adrenal gland of a 15-month-old boy, the adrenal gland of a 4-year-old girl, and the retroperitoneal region of a 13-month-old boy, respectively. Among the three xenografts, TNB9 and TS-N-2*nu* are chemosensitive and multidrug-resistant, respectively.[7] Small pieces of minced tumor were implanted subcutaneously with trochars into the unilateral or bilateral flanks of 5-week-old male Balb/cAJcl-nu mice (Clea Japan, Tokyo, Japan). After tumor implantation, the mice were randomized into groups of three to five and monitored for tumor growth. Tumor weight was calculated according to the formula: tumor weight (mg) = the length of the tumor (mm) × the width of the tumor $(mm)^2 \times 1/2$. Drug treatment was initiated when the tumors weighed approximately 150 mg.

[1]To whom correspondence should be addressed.
E-mail: mkaneko@md.tsukuba.ac.jp

doi: 10.1111/j.1349-7006.2009.01280.x
© 2009 Japanese Cancer Association

Tumor size and mouse body weight were measured every 4 days. The mean relative tumor weight was calculated as follows: the mean tumor weight on day x/the mean tumor weight on day 0 (the initiation of treatment). Animal experiments were carried out in a humane manner after receiving approval from the Institutional Animal Experiment Committee of the University of Tsukuba and in accordance with the University's Regulations for Animal Experiments as well as the Fundamental Guidelines for the Proper Conduct of Animal Experiments and Related Activities in Academic Research Institutions set forth by the Ministry of Education, Culture, Sports, Science, and Technology of Japan.

Treatment with celecoxib and CPT-11. Celecoxib, which was supplied by Pfizer (Groton, CT, USA), was dissolved in dimethyl sulfoxide at 5 mg/mL, further diluted 10 times in 0.5% methylcellulose with 0.025% Tween 20, and administered intraperitoneally (i.p.) at a dose of 5 mg/kg body weight. CPT-11 (Tokyo Chemical Industry, Tokyo, Japan) was injected i.p. at a dose of 5.9 mg/kg body weight (low dose) or 59 mg/kg body weight (conventional dose) in 5% glucose. Celecoxib alone, low-dose CPT-11 alone, or celecoxib in combination with low-dose CPT-11 was each given once daily for 20 consecutive days. Conventional-dose CPT-11 was administered three times at 4-day intervals with or without celecoxib, which was given daily for 12 consecutive days from day 0. Six to eight xenografted tumors for each treatment were used.

Neuroblastoma (NB) cell lines and cell viability assay. *MYCN*-unamplified SK-N-AS and SK-N-SH, and *MYCN*-amplified SK-N-DZ, TGW, and CHP134 cells, were maintained in RPMI-1640 medium supplemented with 10% fetal bovine serum (BioWest, Nuaille, France) and antibiotics at 37°C in a humidified 5% CO_2 atmosphere. Among the five cell lines, SK-N-AS showed chromosome 1p loss, 11q loss, and 17q gain; SK-N-SH demonstrated 17q gain; SK-N-DZ had 11q loss; TGW showed 1p gain, probable 11q loss, and 17q gain; and CHP134 demonstrated 1p loss and 17q gain. Cell viability was determined by a colorimetric 2-(4-indophenyl)-3-(4-nitrophenyl)-5-(2,4-disulfophenyl)-2H-tetrazolium (WST-1) (Dojindo, Kumamoto, Japan) assay. The cells were plated at a density of 5000 cells/well in 96-well tissue culture plates (Becton Dickinson, Franklin Lakes, NJ, USA). After attachment overnight, the cells were incubated with six-step concentrations of celecoxib, SN-38 (an active metabolite of CPT-11) (Yakult Honsha, Tokyo, Japan) or SN-38 combined with 10 μM or 20 μM of celecoxib for 72 hours. The absorbance was measured at 450 nm. All experiments were performed in quadruplicate and repeated three times.

Evaluation of the adverse effects of treatment using the incidence of diarrhea and white blood cell count. Daily diarrheal stool passages were counted for each animal administered with celecoxib and low-dose CPT-11 from days 0 to 19, and for those administered with conventional-dose CPT-11 with or without celecoxib from days 0 to 8. The white blood cell count in the tail vein was performed at 1, 7, and 14 days after the cessation of each therapy.

Immunohistochemistry and detection of apoptotic cell. To detect the Ki-67 nuclear antigen, which is present throughout the cell cycle but absent in the dormant G_0 phase,[19] tumors were fixed in 10% neutral buffered formalin for 24–48 h prior before being embedded in paraffin. After deparaffinization, the tissue sections were heated at 121°C for 15 min in 10 mM Tris-HCl with 1 mM EDTA (pH 9.0). Endogenous peroxidase was blocked with 3% hydrogen peroxide in methanol for 5 min at room temperature. The samples were incubated with anti-Ki-67 antigen, clone MIB-1 (DakoCytomation, Carpinteria, CA, USA), for 60 min at room temperature. To detect CD31, an endothelial cell marker, the tumors were fixed in 0.1 M Tris-HCl (pH 7.4) with 0.05% calcium acetate, 0.5% zinc acetate, and 0.5% zinc chloride for 8 h. After deparaffinization, the tissue sections were covered with 20 μg proteinase K (Wako Pure Chemical Industries, Osaka, Japan)/mL PBS(–) for 30 min at 37°C, followed by incubation with anti-CD31, clone MEC 13.3 (BD Biosciences Pharmingen, Franklin Lakes, NJ, USA), overnight at 4°C. The bound antibodies were amplified using the standard streptavidin–biotin complex immunoperoxidase (ABC) technique (Vector Laboratories, Burlingame, CA, USA). For the coloring reaction, 3,3′-diaminobenzidine (DAB) (Sigma, St Louis, MO, USA) was used as the chromogen, and nuclear counterstaining was carried out with hematoxylin. To assess proliferation, the number of pixels with Ki-67 positively stained nuclei per total number of nuclear pixels was calculated using image analysis software (ImageJ) (NIH, Bethesda, MD, USA) in 15 fields per treatment group at ×150 magnification. The results are expressed as a percentage of the untreated control tumor. The number of CD31 positively stained blood vessels was counted in 20 fields per treatment group at ×300 magnification.

Apoptotic cells in tumor tissues were detected using the TUNEL assay. After deparaffinization, the tissue sections were covered with 20 μg proteinase K/mL PBS(–) for 15 min at room temperature, followed by blocking of endogenous peroxidase activity. The samples were then incubated with TdT enzyme (Takara Bio, Shiga, Japan) and biotin-16-dUTP (Roche Applied Science, Mannheim, Germany) in TdT buffer (Takara Bio) containing 0.01% bovine serum albumin for 1.5 h at 37°C in a humidity chamber. Biotin-16-dUTP nucleotides that had been incorporated into DNA fragments were detected using the ABC method with DAB as the chromogen. The number of TUNEL-positive cells was counted in 20 fields per treatment group at ×150 magnification.

Immunoblotting. Frozen tumor samples were crushed in liquid nitrogen and homogenized in a sample buffer consisting of 125 mM Tris-HCl (pH 6.8), 20 mM dithiothreitol, 4% SDS, 10% glycerol, and 0.5% protease inhibitor cocktail (Complete Mini; Roche Applied Science). The extracts were sonicated for 10 s and centrifuged at 17 000*g* for 10 min at 4°C to remove debris. NB cells were lysed in the sample buffer. The protein concentrations were determined using the Bio-Rad DC protein assay (Bio-Rad Laboratories, Hercules, CA, USA). Samples containing the same amounts of protein were separated by 12.5% or 15% SDS-PAGE, electroblotted on polyvinylidene fluoride membranes (Millipore, Bedford, MA, USA), and probed with antibodies. The primary antibodies used were against COX-2 (Rockland, Gilbertsville, PA, USA), VEGF clone A-20 (Santa Cruz Biotechnology, Santa Cruz, CA, USA), Bcl-2 clone 8C8, Bax clone 2D2, p53 clone DO-1 (Calbiochem, Darmstadt, Germany), caspase-8 clone E7 (Epitomics, Burlingame, CA, USA), caspase-9 clone 5B4 (Medical & Biological Laboratories, Nagoya, Japan), cleaved caspase-3 (Asp175) clone 5A1, phospho-p53 (Ser15) clone 16G8, caspase-7 clone C7 (Cell Signaling Technology, Danvers, MA, USA), and β-actin clone AC-74 (Sigma). Horseradish peroxidase–conjugated antimouse (Amersham Biosciences, Buckinghamshire, UK) or antirabbit antibody (Stressgen, Victoria, BC, Canada) served as secondary antibodies. An enhanced chemiluminescence system (PerkinElmer Life Sciences, Boston, MA, USA) was used for detection.

Statistical analysis. The responses of NB xenografts to celecoxib alone, CPT-11 alone, and CPT-11 in combination with celecoxib were evaluated with respect to tumor growth delay by measuring the mean interval in days required to reach twice the original tumor weight for individual tumors (TD_2). The incidence of diarrhea, the white blood cell count in mice, the proportion of Ki-67 positively stained cells, the number of TUNEL-positive apoptotic cells, and the number of CD31 positively stained blood vessels in tumor sections were expressed as the mean ± SD. The Student's *t*-test or Welch's *t*-test was used to assess the significance of differences between the treatment groups.

doi: 10.1111/j.1349-7006.2009.01280.x
© 2009 Japanese Cancer Association

Results

Antitumor effects of celecoxib and CPT-11. Celecoxib administered i.p. once daily for 20 consecutive days at 5 mg/kg body weight did not prevent the growth of any of the NB xenografts tested (Fig. 1a, Table 1). Treatment with low-dose or conventional-dose CPT-11 alone demonstrated significant tumor growth inhibition against the three NB xenografts ($n = 6$ in each) ($P < 0.01$ compared with the untreated control, Student's t-test). Furthermore, administration of low-dose daily CPT-11 combined simultaneously with very low-dose celecoxib resulted in highly significant suppression of tumor growth in all three xenografts compared not only with low-dose CPT-11 therapy alone but also with the combination therapy of conventional-dose CPT-11 and celecoxib ($P < 0.001$) (Fig. 1, Table 1). In combination therapy involving low-dose CPT-11 and celecoxib, one of six TNB9 tumors, one of six TS-N-5*nu* tumors, and two of eight TS-N-2*nu* tumors weighed less than their original tumor weight at the end of the experiment, at day 100 in TNB9 and TS-N-2*nu* and at day 70 in TS-N-5*nu*. These results demonstrate that prolonged very low-dose administration of celecoxib enhances the antitumor activity of low-dose CPT-11 against NB xenografts, despite the fact that very low-dose celecoxib administration alone has no significant antitumor effect.

Effects of celecoxib and SN-38 on the survival of SK-N-AS, SK-N-DZ, and TGW cells *in vitro*. The IC50s of celecoxib were 50 μM for SK-N-AS, 52 μM for SK-N-DZ, and 60 μM for TGW (Fig. 2, left panels). Combined treatment with 10 μM or 20 μM celecoxib did not enhance cell killing by SN-38 in any cell line irrespective of *MYCN* amplification status and pattern of chromosome gains and losses (Fig. 2 right panels).

Effects of celecoxib and CPT-11 on body weight gain, incidence of diarrhea, and white blood cell count. The body weight of the nude mice did not fall below that at the initiation of treatment for any treatment schedule (Fig. 3). Celecoxib alone caused no diarrhea in the mice (Table 2). CPT-11 induced slight diarrhea with wet and soft stools within 2 h of the injection irrespective of the administered dose. The diarrhea stopped within 6 h. No CPT-11-induced late diarrhea was observed. The percentage of incidence of acute diarrheal episode after the administration of CPT-11 with or without celecoxib was calculated for each animal. Interestingly, daily co-treatment with celecoxib significantly suppressed the incidence of diarrhea induced by daily low-dose CPT-11 ($P = 0.033$ compared with

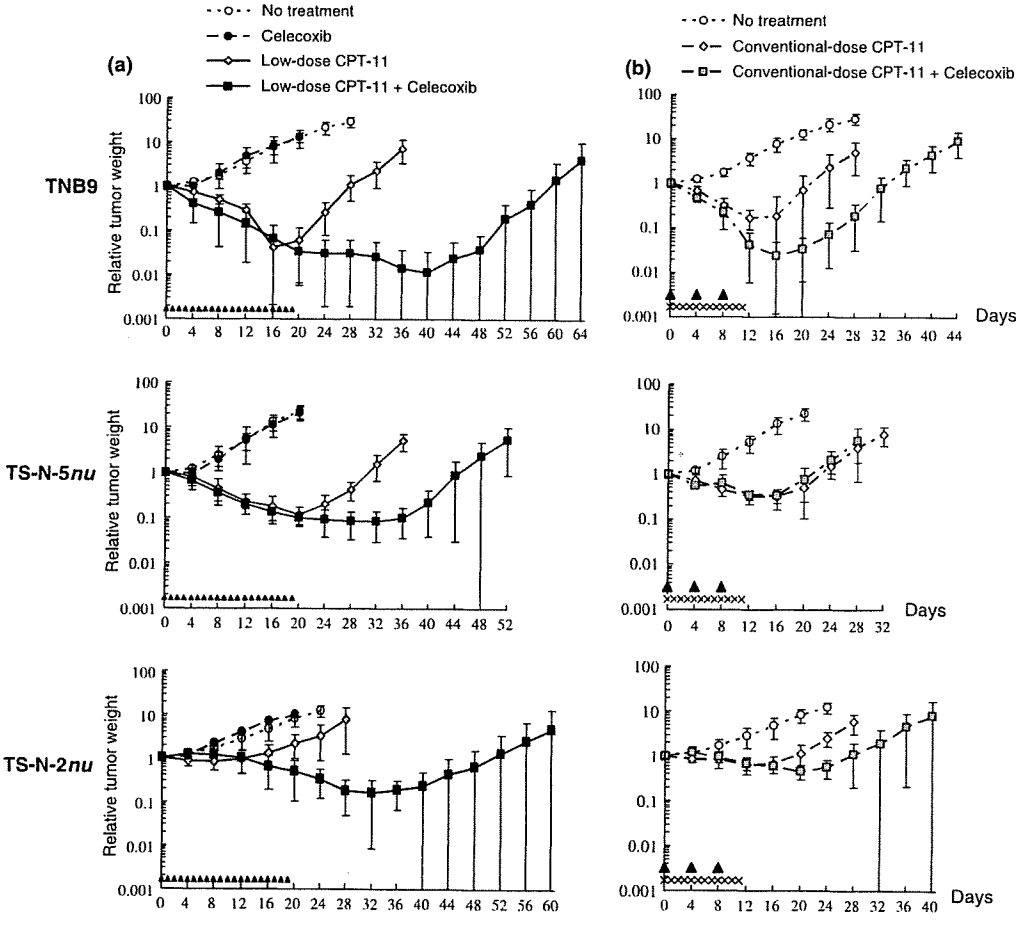

Fig. 1. Responses of TNB9, TS-N-5*nu*, and TS-N-2*nu* xenografts to celecoxib and (a) low-dose irinotecan (CPT-11) and (b) conventional-dose CPT-11. Treatment was initiated on day 0, when the tumors weighed approximately 150 mg. Tumors were measured every 4 days. The results are presented as mean relative tumor weight ± SD to that on day 0. Celecoxib administered i.p. once daily for 20 consecutive days at 5 mg/kg body weight did not significantly prevent the growth of any neuroblastoma (NB) xenograft. Each treatment schedule for CPT-11 alone demonstrated significant tumor growth inhibition against the three NB xenografts. Administration of low-dose daily CPT-11 combined simultaneously with celecoxib resulted in highly significant suppression of tumor growth in all three xenografts compared not only with low-dose CPT-11 therapy alone but also with the combination therapy of conventional-dose CPT-11 and celecoxib. The arrowheads and crosses indicate drug administration.

© 2009 Japanese Cancer Association

Table 1. Tumor doubling times of TNB9, TS-N-5*nu*, and TS-N-2*nu* xenografts treated with irinotecan (CPT-11) and celecoxib

Neuroblastoma xenograft	CPT-11	Celecoxib	TD_2 (days)	*P*-value	
TNB9	—	−	8.9 ± 1.9	*P* = 0.993	
		+	9.0 ± 3.7		
	Low dose	−	31.6 ± 2.7	*P* < 0.0001	*P* < 0.0001
		+	>70.9		
	Conventional dose	−	25.3 ± 3.8	*P* < 0.001	
		+	37.3 ± 4.8		
TS-N-5*nu*	—	−	7.1 ± 1.1	*P* = 0.075	
		+	8.9 ± 2.1		
	Low dose	−	33.1 ± 1.2	*P* < 0.0001	*P* < 0.0001
		+	>51.5		
	Conventional dose	−	25.8 ± 1.9	*P* = 0.272	
		+	24.4 ± 2.2		
TS-N-2*nu*	—	−	10.2 ± 2.6	*P* = 0.767	
		+	9.6 ± 4.7		
	Low dose	−	21.2 ± 4.3	*P* < 0.0001	*P* < 0.001
		+	>82.9		
	Conventional dose	−	23.0 ± 2.4	*P* = 0.0155	
		+	36.0 ± 7.8		

TD_2, mean interval in days required to reach twice the original tumor weight for individual tumors.

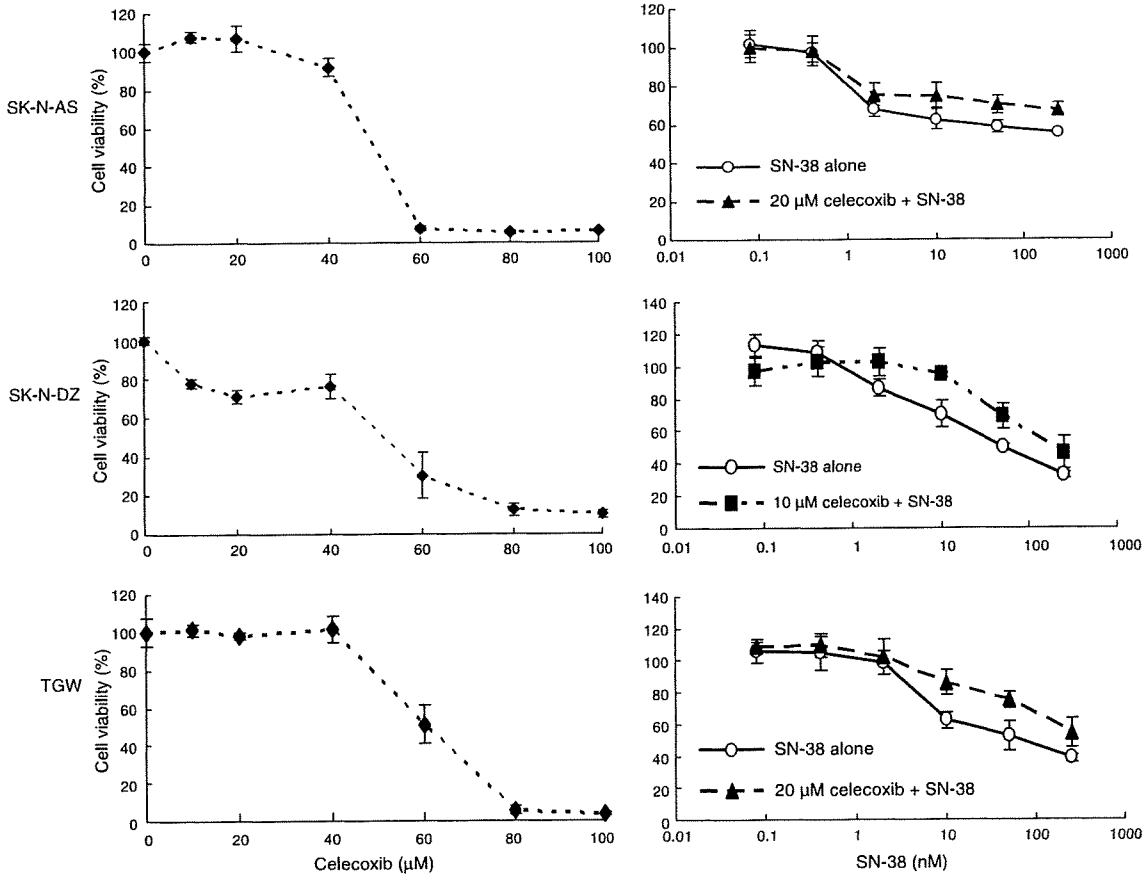

Fig. 2. Effects of celecoxib and SN-38 on the survival of SK-N-AS, SK-N-DZ, and TGW cells *in vitro*. The IC_{50}s of celecoxib were 50 μM for SK-N-AS, 52 μM for SK-N-DZ, and 60 μM for TGW (left panels). Combined treatment with 10 μM or 20 μM celecoxib did not enhance cell killing by SN-38 in any cell line (right panels). The cells were incubated with six-step concentrations of celecoxib, SN-38, or SN-38 combined with 10 μM or 20 μM of celecoxib for 72 hours. Cell viability was determined by the 2-(4-indophenyl)-3-(4-nitrophenyl)-5-(2,4-disulfophenyl)-2H-tetrazolium (WST-1) assay. The results are presented as the mean ± SD.

doi: 10.1111/j.1349-7006.2009.01280.x
© 2009 Japanese Cancer Association

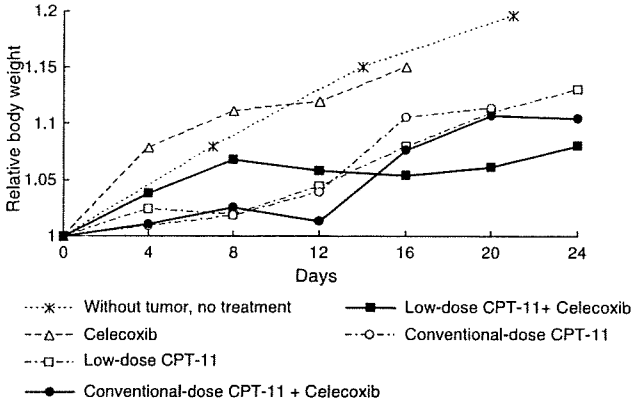

Fig. 3. Body weight changes of mice during the treatments. The body weight of the mice did not fall below that at day 0 for any treatment schedule. The body weights of five untreated mice without tumors were measured every 7 days. Data are presented as the mean body weight relative to that at 6 weeks of age. The mean relative body weight (RBW) for tumor-bearing mice was calculated as follows: RBW = *Bx/Bo*, where *Bx* and *Bo* are the mean values of observed body weight minus the calculated tumor weight of animals that received the same treatment of celecoxib and CPT-11 on days x and day 0, respectively. The results are presented as the mean body weight relative to that on day 0. For simplicity, SD bars are not shown.

low-dose CPT-11 alone, Student's *t*-test) (Table 2). The white blood cell count was significantly reduced 24 h after the cessation of intermittent conventional-dose therapy with CPT-11 with or without celecoxib ($P < 0.01$ compared with the untreated control, Student's *t*-test). No mice died during the experiments.

Tumor cell proliferation in NB xenografts. Tumors from untreated mice and from animals treated with celecoxib alone showed no significant difference in tumor cell proliferation in each NB xenograft (Fig. 4a, Fig 5A, panels a and b). Daily administration of low-dose CPT-11 alone for 10 consecutive days significantly inhibited cell proliferation in both TNB9 and TS-N-5*nu* compared with the untreated control ($P < 0.0001$, Student's *t*-test). TNB9 is sensitive to many anti-tumor drugs including CPT-11. At 24 h after the cessation of the therapy, there was no significant difference in proliferation inhibition between TNB9 tumors treated with CPT-11 alone and those treated with CPT-11 and celecoxib (data not shown). At 96 h after the cessation of the therapy, TNB9 from mice administered with CPT-11 alone was in its re-growth phase and showed increased proliferation of tumor cells. In contrast, in TNB9 treated with CPT-11 and celecoxib, tumor cell proliferation was significantly inhibited compared with CPT-11 treatment alone, even at 96 h after the removal of the drugs ($P < 0.0001$, Welch's *t*-test) (Fig. 4a, Fig. 5A, panels c and d). Tumor cell proliferation in TS-N-5*nu* tumor was significantly decreased by the combination therapy of CPT-11 and celecoxib compared with CPT-11 alone ($P < 0.0001$ Student's *t*-test) (Fig. 4a, Fig. 5A, panels e and f). In TS-N-2*nu*, a multidrug resistant xenograft, no significant decrease in tumor cell proliferation was observed in spite of the longer administration of low-dose CPT-11 (once daily for 15 consecutive days) ($P = 0.780$, Welch's *t*-test). On the other hand, the combination therapy of CPT-11 and celecoxib resulted in a significant inhibition of TS-N-2*nu* tumor cell proliferation when compared not only to the untreated control ($P < 0.0001$, Welch's *t*-test), but also to CPT-11 therapy alone ($P = 0.00036$, Student's *t*-test) (Fig. 4a, Fig. 5A, panels g and h). These findings show that prolonged very low-dose administration of celecoxib enhances the inhibitory effect of low-dose CPT-11 on tumor cell proliferation.

Apoptotic cells and blood vessels in NB xenografts. There was no significant difference between the untreated control tumors and those administered with celecoxib alone in both the number of TUNEL-positive apoptotic cells (Fig. 4b) and the number of CD31-positive blood vessels (Fig. 4c) for any of the NB xenografts. The combination of low-dose CPT-11 and celecoxib significantly induced apoptosis in TS-N-5*nu* compared with CPT-11 therapy alone ($P < 0.0001$, Student's *t*-test) (Fig. 4b, Fig 5B). Apoptotic cell number was significantly different between TNB9 tumors treated with CPT-11 alone and those treated with CPT-11 and celecoxib 96 h after the cessation of the therapy ($P < 0.0001$, Student's *t*-test). Tumor vascularity was significantly decreased in all xenografts treated with CPT-11 alone compared to the untreated control ($P = 0.0046$ for TNB9, $P = 0.0092$ for TS-N-5*nu*, and $P = 0.012$ for TS-N-2*nu*). There was no significant difference in the number of blood vessels between the tumors treated with CPT-11 alone and those treated with CPT-11 and celecoxib in any of three xenografts (Fig. 4c, Fig. 5C). These results demonstrate that prolonged very low-dose celecoxib augments CPT-11-induced apoptosis, but may not be associated with the inhibitory effects of CPT-11 on angiogenesis in NB xenografts.

Table 2. Effects of celecoxib and irinotecan (CPT-11) on the incidence of diarrhea and white blood cell count

Treatment	*n*†	Incidence of acute diarrhea (%)		White blood cell count × $10^2/\mu L$			
					Days after the cessation of the therapy		
					1	7	14
No treatment	4	0		71 ± 13	NA	NA	NA
Celecoxib, qd × 20	3	0			102 ± 24	89 ± 9	87 ± 14
Low-dose CPT-11, qd × 20	3	82 ± 11	$P = 0.033$		93 ± 33	73 ± 20	73 ± 16
Low-dose CPT-11 + Celecoxib, qd × 20	3	52 ± 11			102 ± 13	61 ± 9	99 ± 6
Conventional-dose CPT-11, q4d × 3	3	78 ± 19	$P = 0.230$		30 ± 6‡	52 ± 16	84 ± 16
Conventional-dose CPT-11, q4d × 3 + Celecoxib, qd × 9	3	56 ± 19			28 ± 6‡	73 ± 7	63 ± 11

CPT-11 induced slight diarrhea with wet and soft stools within 2 h of the injection irrespective of the administered dose. The diarrhea stopped within 6 h. No CPT-11-induced late diarrhea was observed. The percentage of incidence of acute diarrheal episode after the administration of CPT-II with or without celecoxib was calculated for each animal. †*n*, the number of nude mice tested; ‡$P < 0.01$ compared with the untreated control by the Student's *t*-test; qd × 9 and qd × 20, administration once daily for 9 and 20 consecutive days, respectively; q4d × 3, administration three times at 4-day intervals. The results are presented as the mean ± SD.

© 2009 Japanese Cancer Association

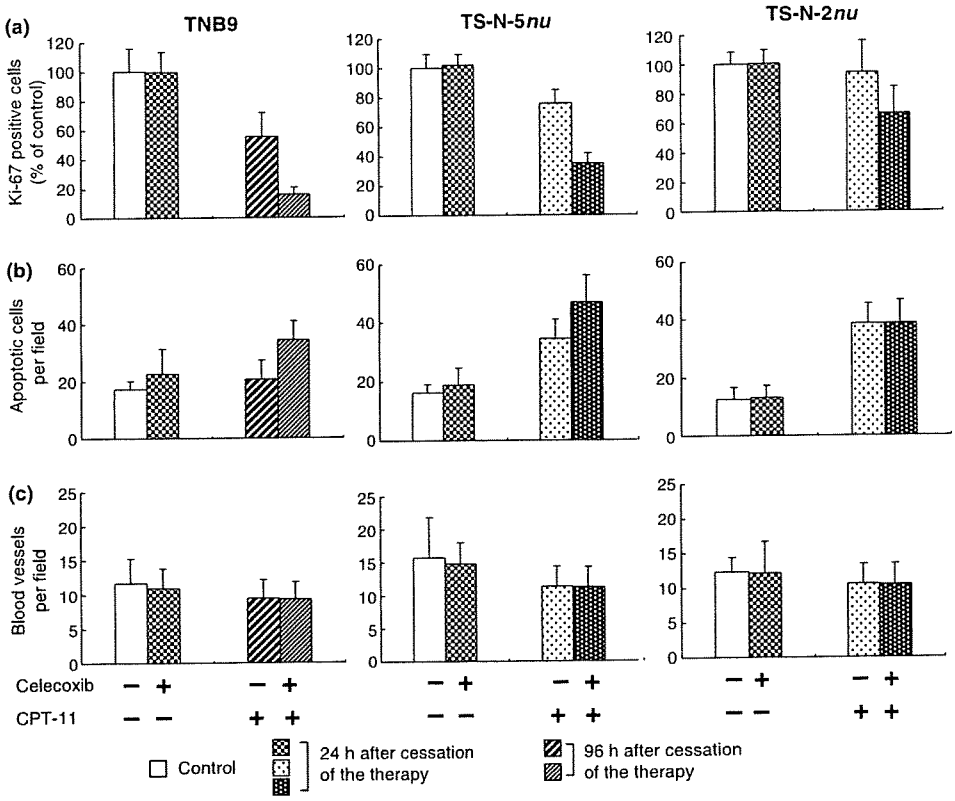

Fig. 4. Prolonged very low-dose administration of celecoxib enhanced the inhibitory effect of low-dose irinotecan (CPT-11) on (a) tumor cell proliferation and (b) CPT-11-induced apoptosis, but might not be associated with (c) its anti-angiogenic effects. Celecoxib alone, low-dose CPT-11 alone, or low-dose CPT-11 in combination with celecoxib were given once daily for 10 consecutive days to mice with the TNB9 or TS-N-5*nu* xenografts and for 15 consecutive days to mice with the TS-N-2*nu* xenograft. To assess tumor cell proliferation, the number of pixels with Ki-67 positively stained nuclei per total number of nuclear pixels was calculated for 15 fields per treatment group at ×150 magnification. The results are expressed as the mean percentage ± SD of the untreated control tumor. The numbers of TUNEL-positive apoptotic cells and CD31-positive blood vessels in the tumor sections were counted in 20 fields per treatment group at ×150 magnification and ×300 magnification, respectively. The results are presented as the mean ± SD.

Protein expression analysis in NB xenografts and NB cells. Protein expression was analyzed in xenografts that had been untreated or treated with CPT-11 and celecoxib once daily for 10 consecutive days for TS-N-2*nu* and for 7 consecutive days for TNB9 and TS-N-5*nu*. The proteins were also analyzed in NB cells untreated or treated *in vitro* with 2 nM SN-38 (for CHP134), 5 nM SN-38 (for SK-N-SH), and 20 μM celecoxib for 72 h. COX-2 protein expression was down-regulated in TS-N-2*nu* administered with CPT-11 and celecoxib, a selective COX-2 inhibitor (Fig. 6a). In the SK-N-AS cells and the TNB9 and TS-N-5*nu* tumors, the expression level of COX-2 protein was low. Caspase-8, which represents the apical caspase in the death receptor pathway, was inactivated during apoptosis in all three xenografts (Fig. 6b). We then investigated the expression of VEGF and apoptosis-related proteins in the mitochondrial pathway in the chemosensitive TNB9 and the multidrug resistant TS-N-2*nu*. VEGF protein expression, which may contribute to tumor angiogenesis, was inhibited by the combination of CPT-11 and celecoxib (Fig. 6c). Administration of CPT-11 with and without celecoxib caused up-regulation of Bax, one of the pro-apoptotic members of Bcl-2 family, and marked down-regulation of Bcl-2, an inhibitor of apoptosis. Combination therapy involving low-dose CPT-11 and celecoxib induced caspase-9 and -7 activation in TNB9 and caspase-9, -7, and -3 activation in TS-N-2*nu*. p53 seemed to be independent of the observed apoptosis. Combined treatment with low concentrations of SN-38 and celecoxib activated caspase 9/7- and 9/3-dependent pathways in the SK-N-SH and CHP134 cells, respectively (Fig. 6D). These results demonstrate that the enhanced antitumor effects of combination therapy involving low-dose CPT-11 and very low-dose celecoxib against NB xenografts may be partially COX-2-independent and are probably mediated through multiple mechanisms including diminished VEGF expression, and activation of the caspase-dependent mitochondrial apoptosis pathway.

Discussion

This is the first *in vivo* report that demonstrates that the antitumor effects of combination therapy involving prolonged low-dose CPT-11 and very low-dose celecoxib against NB xenografts are apparently synergistic without substantial side effects in mice, i.e. much greater than the sum of the effects of each drug administered alone. Daily celecoxib alone administered at a very low dose could not prevent the growth of any of the NB xenografts tested. However, the combination of prolonged low-dose CPT-11 and simultaneous very low-dose celecoxib resulted in highly significant suppression of tumor growth in all three xenografts compared not only with low-dose CPT-11 therapy alone, but also with the combination therapy of intermittent conventional-dose CPT-11 and celecoxib accompanied by decreased proliferation and increased induction of apoptosis in tumor cells. A number of studies have shown additive antitumor efficacy when celecoxib was used in combination with CPT-11 in mouse and rat tumor models.[20,21] In each of these studies,

doi: 10.1111/j.1349-7006.2009.01280.x
© 2009 Japanese Cancer Association

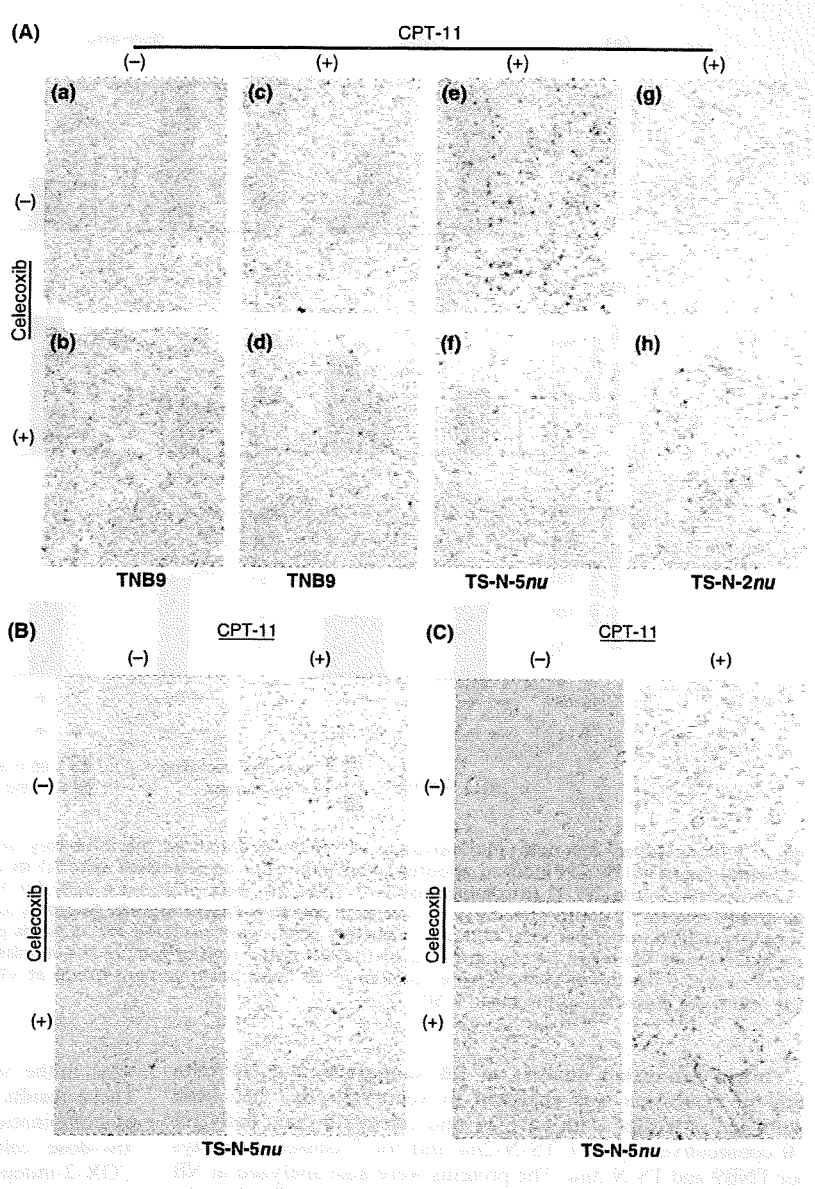

Fig. 5. Immunohistochemistry for Ki-67 antigen, TUNEL, and CD31. (Original magnification, ×150 for A and B; ×300 for C.) (A) (a,b) TNB9 tumors from untreated mice and from animals administered with celecoxib alone showed no difference in tumor cell proliferation. (c,d) At 96 h after the cessation of the therapy, TNB9 tumors from mice administered with low-dose irinotecan (CPT-11) alone were in their regrowth phase and showed increased proliferation of tumor cells. In contrast, in TNB9 treated with low-dose CPT-11 combined with celecoxib, tumor cell proliferation remained inhibited at 96 h after the removal of the drugs. (e,f and g,h) The Ki-67-positive cells in TS-N-5*nu* and TS-N-2*nu* were fewer in number after the combination therapy of low-dose CPT-11 and celecoxib compared with after CPT-11 alone. (B) There was no difference in the number of TUNEL-positive apoptotic cells between the untreated control TS-N-5*nu* tumors and those administered with celecoxib alone. The number of apoptotic cells induced by combined treatment involving low-dose CPT-11 and celecoxib was increased compared with that for CPT-11 alone. (C) Blood vessels in TS-N-5*nu* tumors treated with low-dose CPT-11 were fewer in number than those in untreated and celecoxib-treated tumors. There was no difference in the number of blood vessels between the tumors treated with CPT-11 alone and those treated with CPT-11 and celecoxib.

celecoxib alone administered daily at doses five to 10 times as high as that we used caused tumor growth inhibition. Our results indicate that the administration of prolonged low-dose CPT-11 is essential for achieving enhanced antitumor effects against NB xenografts, and that it is sufficient for celecoxib to be administered daily at a very low dose when combined with prolonged low-dose CPT-11. The *in vitro* WST-1 cell viability assay revealed that low concentrations of celecoxib did not enhance the cytotoxic activity of SN-38 in any of the three cell lines irrespective of their *MYCN* amplification status, patterns of chromosome gains and losses, and COX-2 expression levels. The findings obtained from human NB xenografts in nude mice indicate realistic preclinical data and may be useful in developing treatment for NB. The *in vivo* relationship between genetic background of the NB xenografts and sensitivity to the combined therapy with CPT-11 and celecoxib should further be investigated.

Celecoxib, the first COX-2 specific inhibitor approved for use against osteoarthritis and rheumatoid arthritis, has similar efficacy to conventional nonsteroidal anti-inflammatory drugs in relieving pain and improving functional status, but is associated with a lower incidence of upper gastrointestinal ulceration and complications.[22,23] Recently, data suggesting an increased cardiovascular risk associated with the use of celecoxib have been reported.[24,25] However, other papers have demonstrated that both COX-specific and non-specific inhibitors may increase the risk of serious cardiovascular events, but that celecoxib therapy is associated with increased cardiovascular risk only when used at doses substantially higher than those recommended for the treatment of arthritis.[26–29] COX-2 is overexpressed in many human tumors and promotes tumor progression, suggesting that COX-2 inhibition may be beneficial for cancer treatment, while recent studies have demonstrated that dimethylcelecoxib, a derivative of celecoxib that lacks its COX-2-inhibitory function, potently mimics the antitumor effects of celecoxib on Burkitt's lymphoma, multiple myeloma, and glioblastoma *in vitro* and *in vivo*.[30–32] The sensitivity of NB cells to celecoxib *in vitro* seemed to be independent of their COX-2 protein expression levels. The combination of low-dose CPT-11 and very low-dose celecoxib highly suppressed tumor growth irrespective of the expression level of COX-2 protein compared with CPT-11 therapy alone. The enhanced antitumor effect of the combination

© 2009 Japanese Cancer Association

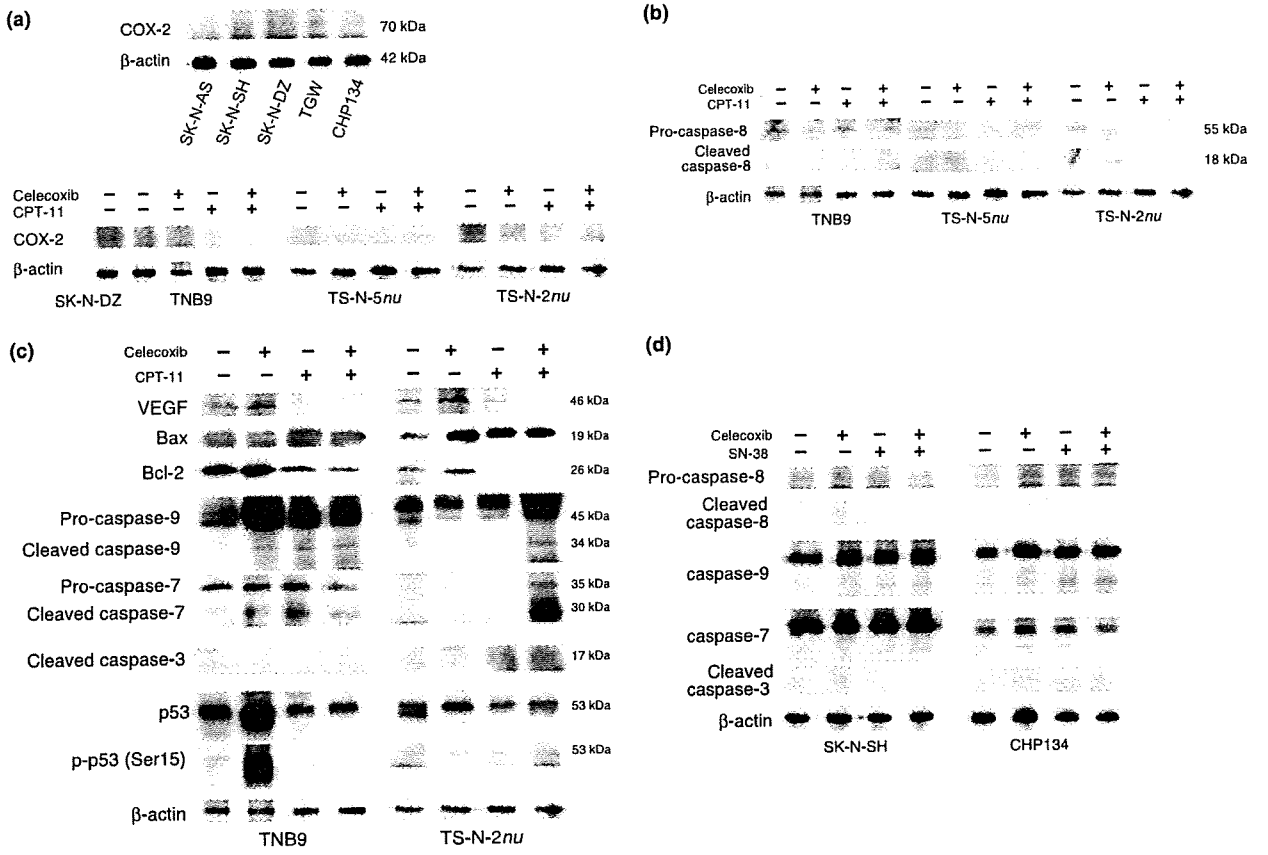

Fig. 6. Immunoblot analysis in neuroblastoma (NB) xenografts and NB cell lines. Tumors that had been untreated or treated with drugs once daily for 10 consecutive days for TS-N-2*nu* and for 7 consecutive days for TNB9 and TS-N-5nu were crushed in liquid nitrogen and lysed in a sample buffer. NB cells were lysed in the sample buffer. Western blot analysis was performed as described in "Materials and Methods". Immunoblotting for β-actin demonstrated equivalent protein loading. (a) Cyclooxygenase (COX)-2 protein expression in NB cells and NB xenografts. The expression of COX-2 in SK-N-DZ cells was used as a positive control. (b) Caspase-8 protein expression in TNB9, TS-N-5*nu*, and TS-N-2*nu* xenografts. (c) Expression of VEGF and apoptosis-related proteins in the mitochondrial pathway in the chemosensitive TNB9 and the multidrug resistant TS-N-2*nu*. VEGF, vascular endothelial growth factor; Bax, Bcl-2-associated X protein; Bcl-2, B cell lymphoma/leukemia-2; p-p53 (Ser15), phospho-p53 at Ser15. (d) Protein expression of caspase-8, -9, -7, and -3 in SK-N-SH and CHP134 cells. The cells were incubated with 5 nM SN-38 (for SK-N-SH), 2 nM SN-38 (for CHP134), and 20 μM celecoxib for 72 h.

of the two drugs against NB xenografts is at least partially COX-2-independent and is probably mediated through multiple factors including diminished expression of VEGF and activation of the caspase-dependent mitochondrial apoptosis pathway.

Treatment with low-dose CPT-11 alone resulted in significantly decreased tumor vascularity, whereas the combination of low-dose CPT-11 and very low-dose celecoxib led to no more inhibition of angiogenesis. Eggert *et al.*[33] showed that high gene expression levels of seven angiogenic factors, including VEGF, are strongly correlated with advanced-stage NB. They suggested that the inhibition of VEGF bioactivity alone might not be sufficient for anti-angiogenic therapy for human NB.

Acknowledgments

We thank Dr. Akira Nakagawara, Dr. Miki Ohira, and Dr. Yohko Nakamura in the Chiba Cancer Center Research Institute for providing chromosomal data on the NB cell lines. This work was supported in part by a Grant-in-Aid for Exploratory Research (KAKENHI no. 19659456) and a Grant-in-Aid for Scientific Research (A) (KAKENHI no. 19209054) from the Ministry of Education, Culture, Sports, Science, and Technology of Japan.

References

1 Inagaki J, Yasui M, Sakata N *et al.* Successful treatment of chemoresistant stage 3 neuroblastoma using irinotecan as a single agent. *J Pediatr Hematol Oncol* 2005; **27**: 604–6.
2 Shitara T, Shimada A, Hanada R *et al.* Irinotecan for children with relapsed solid tumors. *Pediatr Hematol Oncol* 2006; **23**: 103–10.
3 Kushner BH, Kramer K, Modak S *et al.* Irinotecan plus temozolomide for relapsed or refractory neuroblastoma. *J Clin Oncol* 2006; **24**: 5271–6.
4 Kiyota N, Tahara M, Fujii S *et al.* Nonplatinum-based chemotherapy with irinotecan plus docetaxel for advanced or metastatic olfactory neuroblastoma: a retrospective analysis of 12 cases. *Cancer* 2008; **112**: 885–91.
5 Bomgaars LR, Bernstein M, Krailo M *et al.* Phase II trial of irinotecan in children with refractory solid tumors: a Children's Oncology Group Study. *J Clin Oncol* 2007; **25**: 4622–7.
6 Vassal G, Giammarile F, Brooks M *et al.* A phase II study of irinotecan in children with relapsed or refractory neuroblastoma: a European cooperation of the Société Française d'Oncologie Pédiatrique (SFOP) and the United Kingdom Children Cancer Study Group (UKCCSG). *Eur J Cancer* 2008; **44**: 2453–60.
7 Kaneko S, Ishibashi M, Kaneko M. Vascular endothelial growth factor expression is closely related to irinotecan-mediated inhibition of tumor

doi: 10.1111/j.1349-7006.2009.01280.x
© 2009 Japanese Cancer Association

growth and angiogenesis in neuroblastoma xenografts. *Cancer Sci* 2008; **99**: 1209–17.
8 Taketo MM. Cyclooxygenase-2 inhibitors in tumorigenesis (Part 1). *J Natl Cancer Inst* 1998; **90**: 1529–36.
9 Hung WC. Anti-metastatic action of non-steroidal anti-inflammatory drugs. *Kaohsiung J Med Sci* 2008; **24**: 392–7.
10 Pai R, Soreghan B, Szabo IL *et al.* Prostaglandin E2 transactivates EGF receptor: a novel mechanism for promoting colon cancer growth and gastrointestinal hypertrophy. *Nat Med* 2002; **8**: 289–93.
11 Tsujii M, Kawano S, Tsuji S *et al.* Cyclooxygenase regulates angiogenesis induced by colon cancer cells. *Cell* 1998; **93**: 705–16.
12 Lin MT, Lee RC, Yang PC *et al.* Cyclooxygenase-2 inducing Mcl-1-dependent survival mechanism in human lung adenocarcinoma CL1.0 cells. Involvement of phosphatidylinositol 3-kinase/Akt pathway. *J Biol Chem* 2001; **276**: 48997–9002.
13 Costa C, Soares R, Reis-Filho JS *et al.* Cyclo-oxygenase 2 expression is associated with angiogenesis and lymph node metastasis in human breast cancer. *J Clin Pathol* 2002; **55**: 429–34.
14 Koki AT, Masferrer JL. Celecoxib: a specific COX-2 inhibitor with anticancer properties. *Cancer Control* 2002; **9**: 28–35.
15 Johnsen JI, Lindskog M, Ponthan F *et al.* Cyclooxygenase-2 is expressed in neuroblastoma, and nonsteroidal anti-inflammatory drugs induce apoptosis and inhibit tumor growth *in vivo*. *Cancer Res* 2004; **64**: 7210–5.
16 Thun MJ, Henley SJ, Patrono C. Nonsteroidal anti-inflammatory drugs as anticancer agents: mechanistic, pharmacologic and clinical issues. *J Natl Cancer Inst* 2002; **94**: 252–66.
17 Gasparini G, Longo R, Sarmiento R *et al.* Inhibitors of cyclo-oxygenase 2: a new class of anticancer agents? *Lancet Oncol* 2003; **4**: 605–15.
18 Gately S, Kerbel R. Therapeutic potential of selective cyclooxygenase-2 inhibitors in the management of tumor angiogenesis. *Prog Exp Tumor Res* 2003; **37**: 179–92.
19 Gerdes J, Lemke H, Baisch H *et al.* Cell cycle analysis of a cell proliferation-associated human nuclear antigen defined by the monoclonal antibody Ki-67. *J Immunol* 1984; **133**: 1710–5.
20 Trifan OC, Durham WF, Salazar VS *et al.* Cyclooxygenase-2 inhibition with celecoxib enhances antitumor efficacy and reduces diarrhea side effect of CPT-11. *Cancer Res* 2002; **62**: 5778–84.
21 Ponthan F, Wickström M, Gleissman H *et al.* Celecoxib prevents neuroblastoma tumor development and potentiates the effect of chemotherapeutic drugs in vitro and in vivo. *Clin Cancer Res* 2007; **13**: 1036–44.
22 Emery P, Zeidler H, Kvien TK *et al.* Celecoxib versus diclofenac in long-term management of rheumatoid arthritis: randomized double-blind comparison. *Lancet* 1999; **354**: 2106–11.
23 Clemett D, Goa KL. Celecoxib: a review of its use in osteoarthritis, rheumatoid arthritis and acute pain. *Drugs* 2000; **59**: 957–80.
24 Solomon SD, McMurray JJ, Pfeffer MA *et al.* Cardiovascular risk associated with celecoxib in a clinical trial for colorectal adenoma prevention. *N Engl J Med* 2005; **352**: 1071–80.
25 Solomon SD, Wittes J, Finn PV *et al.* Cardiovascular risk of celecoxib in 6 randomized placebo-controlled trials: the cross trial safety analysis. *Circulation* 2008; **117**: 2104–13.
26 White WB, Faich G, Borer JS *et al.* Cardiovascular thrombotic events in arthritis trials of the cyclooxygenase-2 inhibitor celecoxib. *Am J Cardiol* 2003; **92**: 411–8.
27 Caldwell B, Aldington S, Weatherall M *et al.* Risk of cardiovascular events and celecoxib: a systematic review and meta-analysis. *J R Soc Med* 2006; **99**: 132–40.
28 McGettigan P, Henry D. Cardiovascular risk and inhibition of cyclo-oxygenase: a systematic review of the observational studies of selective and nonselective inhibitors of cyclooxygenase 2. *JAMA* 2006; **296**: 1633–44.
29 Howes LG. Selective COX-2 inhibitors, NSAIDs and cardiovascular events – is celecoxib the safest choice? *Ther Clin Risk Manag* 2007; **3**: 831–45.
30 Kardosh A, Wang W, Uddin J *et al.* Dimethyl-celecoxib (DMC), a derivative of celecoxib that lacks cyclooxygenase-2-inhibitory function, potently mimics the anti-tumor effects of celecoxib on Burkitt's lymphoma in vitro and in vivo. *Cancer Biol Ther* 2005; **4**: 571–82.
31 Kardosh A, Soriano N, Liu YT *et al.* Multitarget inhibition of drug-resistant multiple myeloma cell lines by dimethyl-celecoxib (DMC), a non-COX-2 inhibitory analog of celecoxib. *Blood* 2005; **106**: 4330–8.
32 Pyrko P, Soriano N, Kardosh A *et al.* Downregulation of survivin expression and concomitant induction of apoptosis by celecoxib and its non-cyclooxygenase-2-inhibitory analog, dimethyl-celecoxib (DMC), in tumor cells in vitro and in vivo. *Mol Cancer* 2006; **5**: 19–34.
33 Eggert A, Ikegaki N, Kwiatkowski J *et al.* High-level expression of angiogenic factors is associated with advanced tumor stage in human neuroblastomas. *Clin Cancer Res* 2000; **6**: 1900–8.

© 2009 Japanese Cancer Association

Japanese Society of Pediatric Surgeons (JSPS)

初回治療後38年後に腹部腫瘤を指摘された病期3後腹膜原発神経芽腫群腫瘍の症例

金子 道夫*

要 旨

39歳の女性が右季肋部痛で受診，超音波検査で肝脾腫とともに上腹部に大きな腫瘤が発見された．生後9か月に後腹膜神経芽腫の診断で東大にて治療を受けたことから筑波大に紹介された．乳児期はVMA陽性，腫瘤は切除不能で生検にて分化傾向のある神経節芽腫と診断され（今回中央病理診断に提出；神経芽腫低分化型 low MKI，INPC favorable histology），化学療法・放射線治療後に手術を行ったが切除不能であった．術後化学療法後中学卒業までフォローされた．結婚して2児をもうけている．当院の検査では腫瘤内を腹腔動脈，上腸間膜動脈が貫通し充実性の腫瘍は悪性腫瘍を思わせるが，VMA，HVA，NSEすべて正常 MIBG取り込みなく，経過観察とした．その後肝硬変が進行して肝移植を考慮しているが，後腹膜腫瘍は変化が見られず，生検未施行だが神経節腫である可能性が極めて高い．一方，小児期に受けた放射線治療により皮膚移植を必要とした皮膚障害と肋骨消失が見られた．これだけ長期間にわたり大きな腫瘤のままであった神経節腫の報告はなく，診断治療の上で重要な症例である．

索引用語：神経節腫，乳児期神経芽腫，incidentaloma，放射線治療

I はじめに

乳児期神経芽腫の自然退縮，成熟化は今では広く知られている．切除不能神経芽腫の治療後38年経ってから腹部腫瘤を指摘され，ほとんど縮小せずに切除困難なままであった症例を経験した．乳児期神経芽腫の治療に関して非常に示唆に富む神経節腫症例と考えられるので報告する．

II 症 例

1．患 者

39歳女性．

2．既 往 歴

1969年1月（9か月）下痢で発症，臍部がやや突出していることに母親が気付いた．2月近医を受診して腹部腫瘤を指摘され，東大小児科を紹介された．経静脈的腎盂造影（IVP）では異常なく，VMA定性試験は陽性で神経芽腫を強く疑われ，開腹手術が行われた．腫瘤は後腹膜原発で肝十二指腸靱帯を後方から圧迫し，胆嚢は緊満していた．腫瘍は腎上極から下極の高さまでみられ，術中下大静脈造影で下大静脈は造影されず，腹部大動脈も腫瘤の中を走行していると判断した．摘出不能で，生検のみとし，術後化学療法のため腹部大動脈にカテーテルが挿入された．後腹膜に両側にまたがる原発巣およびリンパ節転移で遠隔転移はなく病期Ⅲであった．術後動脈より vincristine，静脈より daunorubicin が，1週ごとに交互に投与された．また，腹部の8×10 cmの照射野に220 kVのX線照射がtotal 30 Gy施行された．縮小効果は軽度で，7月の再手術も生検に終わった．前回の生検組織より神経節細胞への分化が認められ，病理診断は“ganglioneuroblastoma in differentiation”であった．退院までに VCR（0.5 mg）9回，cyclophosphamide（100 mg）5回，daunorubicin（6.3 mg）5回投与した．外来で James 療法が行われたが期間・総投与量は不明である．

腹部皮膚が広範に放射線皮膚炎後のケロイドとなり，1981年（13歳）にケロイド除去，皮膚移植を施行した．中学卒業まで東大小児科でフォローされた．その後結婚し，2児の母親となり，子供には特に問題はない．腹部

* 筑波大学臨床医学系小児外科
（〒305-8575 つくば市天王台 1-1-1）

NII-Electronic Library Service

Japanese Society of Pediatric Surgeons (JSPS)

腫瘤に関して医療機関を受診したことは全くなかった．

3．現 病 歴

2007年11月（39歳）右季肋部痛で他院内科受診，腹部超音波検査で肝脾腫を認めた．さらに上腹部正中から肝門部にかけて直径6 cmの球形の腫瘤を認めた．CTにて後腹膜に，腹腔動脈，上腸間膜動脈を巻き込んだ6×8 cmの腫瘤があり，腹水も認めた．乳児期に神経芽腫の治療を受けた既往があり，腫瘤の診断および治療方針決定のため当科を紹介された．腹部に放射線照射による皮膚障害後の肥厚性瘢痕に対して行った10×14 cmの長方形の皮膚移植瘢痕（図1）があり，照射野内の肋骨組織は萎縮していた．肝は肋骨弓下に2 cm触知し，辺縁鈍で明らかに硬化していた．

前医のCTでは腫瘍は充実性で石灰化はほとんどなく，一見活動性の悪性腫瘍に見えた．大動脈は左側方へ，下大静脈はやや上方へ偏位しているが，腫瘍外にあり巻き込まれてはいなかった．しかし，腹腔動脈・上腸間膜動脈は腫瘍の中を貫通していた．腫瘍の大部分は血流が少なく，一部に造影効果が見られる部分もあった（図2）．CTでは内部構造ははっきりしなかったが，当院でのMRIでは腫瘍内部に直径3 cmの結節が見られ，また内部は不均一で複雑な隔壁構造が見られた（図3）．腫瘍マーカーは尿中VMA 5.0 mg/gCr，HVA 5.1 mg/gCr, NSE 8.8 ng/ml，LDH 181 IU/*l*と正常，^{123}I-MIBGの取り込みは認めなかった．東大での手術記事と比較すると，ほとんど腫瘤の占拠部位に変化はなく，相対的な大きさは変化しなかったと判断した．肝は明らかに硬変像があり，脾腫も見られた．腹水は肝硬変によるものと考えた．

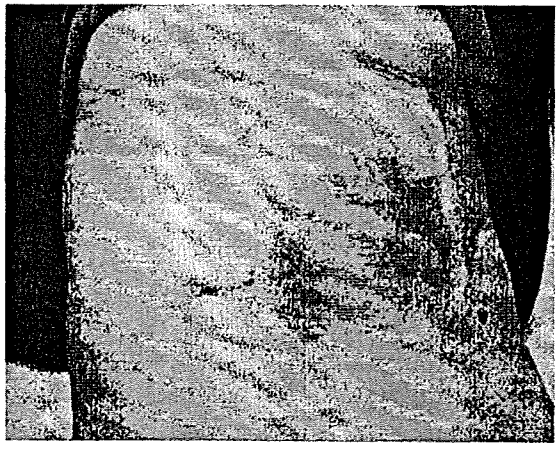

図1 当院初診時の腹部所見

左上腹部を中心に皮膚移植が行われていた．照射野を推定させる．左肋骨弓は照射のため消失していた．

以上より乳幼児期に化学療法・放射線治療を受けた神経芽腫が成熟化し，神経節腫になった可能性が高いと判断し，肝硬変の精査を行いながら経過観察とした．2か月後に造影CTを施行したが，大きさ，性状に変化はなかった．肝硬変の原因として乳児期に輸血を行っていることからウィルスの検索を行ったがすべて陰性であった．抗核抗体は陰性，抗ミトコンドリア抗体も陰性であった．2008年9月に急速な腹水増加と胸水貯留が見られた．さらに，2009年2月食道静脈瘤破裂で緊急入院しEVLで止血した．肝移植の適応があるとして東大病院内科に入院し肝生検を含めた精査の結果，原因不明の非アルコール性脂肪肝炎NASHが最も考えられるとの結論になった．

筑波大学初診時から20か月経過し腫瘍の増大，腫瘍マーカーの上昇は見られず，当初の診断通り神経節腫と考えられた．東大移植外科より後腹膜に悪性を示唆する

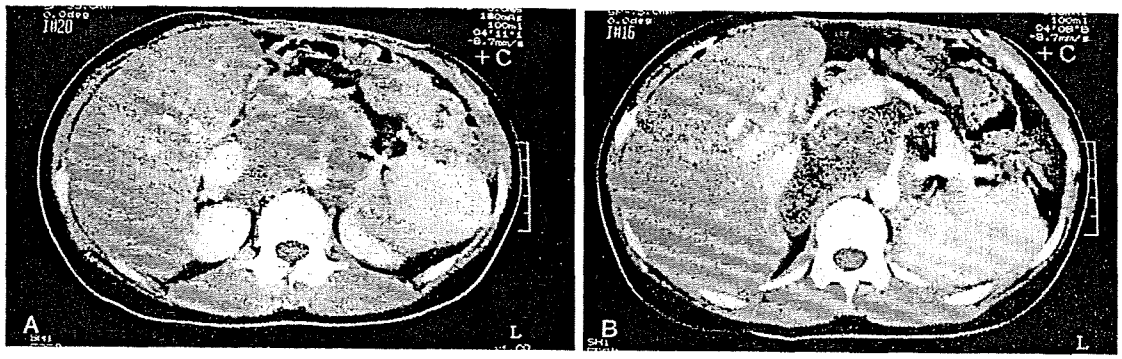

図2 前医での造影CT

腫瘍内は比較的均一だが，ほとんど造影されない．上腸間膜動脈（図2A），腹腔動脈（図2B）は腫瘍の中を貫通している．

NII-Electronic Library Service